

This discussion paper is/has been under review for the journal Atmospheric Measurement Techniques (AMT). Please refer to the corresponding final paper in AMT if available.

Carbon monoxide total columns from SCIAMACHY 2.3 μm atmospheric reflectance measurements: towards a full-mission data product (2003–2012)

T. Borsdorff¹, P. Tol¹, J. E. Williams², J. de Laat², J. aan de Brugh¹, P. Nédélec³, I. Aben¹, and J. Landgraf¹

¹SRON Netherlands Institute for Space Research, Utrecht, the Netherlands

²Royal Netherlands Meteorological Institute (KNMI), de Bilt, the Netherlands

³Laboratoire d'aérologie (LA), CNRS UMR-5560 et Observatoire Midi-Pyrénées, Université Paul-Sabatier, Toulouse, France

Received: 10 August 2015 – Accepted: 3 September 2015 – Published: 17 September 2015

Correspondence to: T. Borsdorff (t.borsdorff@sron.nl)

Published by Copernicus Publications on behalf of the European Geosciences Union.

Abstract

We present a full-mission data product of carbon monoxide (CO) vertical column densities using the 2310–2338 nm SCIAMACHY reflectance measurements over clear sky land scenes for the period January 2003–April 2012. The retrieval employs the SICOR 5 algorithm, which will be used for operational data processing of the Sentinel-5 Precursor mission, combined with a SCIAMACHY specific radiometric soft-calibration to mitigate instrumental issues. The retrieval approach infers simultaneously carbon monoxide, methane and water vapour column densities together with a Lambertian surface albedo from individual SCIAMACHY measurements employing a non-scattering radiative transfer model. To account for the radiometric instrument degradation including the 10 formation of an ice-layer on the 2.3 μm detector-array, we consider clear sky measurements over the Sahara as a natural calibration target. For these specific measurements, we spectrally calibrate the SCIAMACHY measurements and determine a spectral radiometric offset and the width of the instrument spectral response function as a function 15 of time for the entire operational phase of the mission. We show that the smoothing error of individual clear sky CO retrievals is less than ± 1 ppb and thus this error contribution has not to be accounted for in the validation considering the much higher retrieval noise. The CO data product is validated against measurements of ground-based Fourier transform infrared spectrometers at 27 stations of the NDACC-IRWG 20 and TCCON network and MOZAIC/AGOS aircraft measurements at 26 airports worldwide. Overall, we find a good agreement with TCCON measurements with a mean bias $\bar{b} = -1.2$ ppb and a station-to-station bias with $\bar{\sigma} = 7.2$ ppb. For the NDACC-IRWG network, we obtain a larger mean station bias of $\bar{b} = -9.2$ ppb with $\bar{\sigma} = 8.1$ ppb and for the MOZAIC/AGOS measurements we find $\bar{b} = -6.4$ ppb with $\bar{\sigma} = 5.6$ ppb. The SCIA- 25 MACHY data set is subject to a small but significant trend of 1.47 ± 0.25 ppb yr^{-1} . After trend correction, the bias with respect to MOZAIC/AGOS observation is 2.5 ppb, with respect to TCCON measurements it is -4.6 ppb and with respect to NDACC-IRWG measurements -8.4 ppb. Hence, a discrepancy of 3.8 ppb remains between the

[Title Page](#)[Abstract](#)[Introduction](#)[Conclusions](#)[References](#)[Tables](#)[Figures](#)[◀](#)[▶](#)[Back](#)[Close](#)[Full Screen / Esc](#)[Printer-friendly Version](#)[Interactive Discussion](#)

global biases with NDACC-IRWG and TCCON, which is confirmed by directly comparing NDACC-IRWG and TCCON measurements. Generally, the scatter of the individual SCIAMACHY CO retrievals is high and dominated by large measurement noise. Hence, for practical usage of the dataset, averaging of individual retrievals is required. As an example, we show that monthly mean SCIAMACHY CO retrievals, averaged separately over Northern and Southern Africa, reflect the spatial and temporal variability of biomass burning events in agreement with the global chemical transport model TM5.

1 Introduction

Carbon monoxide (CO) is an important atmospheric trace gas for the understanding of tropospheric chemistry and air quality. Its main source is incomplete combustion of fossil fuel and biomass and the oxidation of atmospheric methane and other hydrocarbons. The reaction of CO with the OH radical represents its major atmospheric sink and thus CO regulates the self cleaning capability of the atmosphere (Spivakovsky et al., 2000). Enhanced CO concentration can indicate anthropogenic air pollution (Logan et al., 1981) and as a precursor of ozone (O_3) formation it influences tropospheric air quality (Seiler and Fishman, 1981). Moreover, by constraining the depletion of methane (CH_4), CO affects indirectly global warming (Daniel and Solomon, 1998) and due to its moderate long life time of several weeks to several months (Holloway et al., 2000), it is a tracer for global transport and redistribution of pollutants in the atmosphere (e.g. Yurganov et al., 2004, 2005; Gloudemans et al., 2006).

The global concentration of CO has been measured by various satellite missions (e.g. Clerbaux et al., 2008; Deeter et al., 2003). The Scanning Imaging Absorption Spectrometer for Atmospheric Cartography (SCIAMACHY) was one of the first space-based instruments observing CO from the shortwave infrared (SWIR) range around $2.3\text{ }\mu\text{m}$ (Bovensmann et al., 1999) and it was fully operational from January 2003 until April 2012 when the contact to its host ENVISAT was lost. In this period, an almost continuous long-term record of more than 9 years of SWIR measurements in the $2.3\text{ }\mu\text{m}$

SCIAMACHY CO total column measurements (2003–2012)

T. Borsdorff et al.

Title Page	
Abstract	Introduction
Conclusions	References
Tables	Figures
◀	▶
◀	▶
Back	Close
Full Screen / Esc	
Printer-friendly Version	
Interactive Discussion	



SCIAMACHY CO total column measurements (2003–2012)

T. Borsdorff et al.

[Title Page](#)[Abstract](#)[Introduction](#)[Conclusions](#)[References](#)[Tables](#)[Figures](#)[◀](#)[▶](#)[◀](#)[▶](#)[Back](#)[Close](#)[Full Screen / Esc](#)[Printer-friendly Version](#)[Interactive Discussion](#)

spectral range from space has been recorded. For cloud-free scenes, these spectra are sensitive to the total column density of CO with a good vertical sensitivity throughout the whole atmosphere (Buchwitz et al., 2004; Gloudemans et al., 2008).

In recent years, several algorithms have been developed to infer CO total columns from SCIAMACHY's SWIR measurements (e.g. IMAP-DOAS (Frankenberg et al., 2005), WFM-DOAS (Buchwitz et al., 2004), and IMLM (Gloudemans et al., 2009)). The global CO fields were used for a suite of applications, e.g. the detection of biomass burning events (Buchwitz et al., 2004), to study the inter-annual variability of CO on the global scale (Gloudemans et al., 2009), to investigate pollution patterns of megacities (Buchwitz et al., 2007) and the long range transport of CO in the Southern Hemisphere (Gloudemans et al., 2009), which indicates the broad scope of different application for this data product. Furthermore, the SCIAMACHY CO measurements were compared with corresponding MOPITT CO retrievals (de Laat et al., 2010a) and additionally validated with CO observations of ground-based spectrometers (de Laat et al., 2010b) and MOZAIC/IAGOS aircraft measurements (de Laat et al., 2012). All these previous studies were dedicated to the early years of the mission before 2009. The extensive degradation of the instrument (Gloudemans et al., 2008), caused by the growing ice layer on the detector array and a considerable loss of detector pixels due to radiation damage in the later years of the mission. This reduces the radiometric quality of the SCIAMACHY spectra, which seriously complicates the processing of a SCIAMACHY CO product for the entire mission period.

The Tropospheric Monitoring Instrument (TROPOMI) on board of the Sentinel 5 Precursor (SP-5) mission is expected to be launched in 2016. TROPOMI covers the same 2.3–2.4 μm spectral range as SCIAMACHY with the same spectral resolution but with an improved radiometric performance and a better spatial resolution of the TROPOMI instrument. For the S5-P mission, the highly efficient Shortwave Infrared Carbon Monoxide Retrieval algorithm (SICOR) (Vidot et al., 2012) was developed to meet the demanding requirements of operational data processing regarding calculation time. In this study, we apply the SICOR algorithm to the SWIR measurements of

the SCIAMACHY instrument and infer a data set of CO vertical columns for the entire ENVISAT mission (2003–2012), limited to land and cloud free scenes. This study represents the first application of the TROPOMI operational processor to real data.

Due to unexpected in-orbit problems of the SCIAMACHY measurements in the 5 2.3 µm spectral range (Gloudemans et al., 2005), recalibration of the radiometric measurements is needed. For this purpose, we use clear sky measurements over the Sahara as a natural calibration target in combination with accurate a priori knowledge of the atmospheric methane abundances in this region. For the entire mission lifetime, we determine the temporal dependence of the spectral calibration, a spectral radio-
10 metric offset, and the width of the instrument spectral response function from these measurements. Furthermore, we use SCIAMACHY's solar measurements to obtain a proper reflectance retrieval. Here, multiplicative radiometric errors common to both the radiance and irradiance measurement cancel out and are thus not relevant for the retrieval. Finally, the CO dataset is validated with ground-based TCCON and NDACC-
15 IRWG measurements at 27 sites and MOZAIC/IGAGOS aircraft measurements close to 26 airports.

Averaging of individual SCIAMACHY CO retrievals is essential for data usage to reduce the retrieval noise to an acceptable level. The required degree of averaging depends on the properties of the considered ground scene and the measurement geometry of the instrument. To illustrate potential data use, we compare the spatial and temporal variation of SCIAMACHY CO fields over biomass burning areas in Africa with model fields of a global chemistry transport model (TM5). Choosing an appropriate balance between temporal and spatial averaging of individual SCIAMACHY retrievals allows us to obtain useful information about the atmospheric CO concentration.

25 The paper is organised as follows: Sect. 2 summarises the inversion approach and in Sect. 3 we discuss the degradation of SCIAMACHY instrument and propose mitigation approach. The validation of the CO data product against NDACC-IRWG, TCCON and MOZAIC/IGAGOS measurements is discussed in Sects. 4 and 5 illustrates potential data

SCIAMACHY CO total column measurements (2003–2012)

T. Borsdorff et al.

[Title Page](#)

[Abstract](#)

[Introduction](#)

[Conclusions](#)

[References](#)

[Tables](#)

[Figures](#)

◀

▶

[Back](#)

[Close](#)

[Full Screen / Esc](#)

[Printer-friendly Version](#)

[Interactive Discussion](#)



usage showing a comparison with CO model fields that are simulated by the TM5 global chemistry transport model. Finally, Sect. 6 summarises and concludes the paper.

2 Retrieval approach

To obtain CO vertical column densities, we use SCIAMACHY SWIR measurements in the spectral range 2310.7–2338.4 nm with a spectral resolution of 0.2 nm and a spectral sampling distance of 0.1 nm. The retrieval is based on the profile scaling approach, which was first applied by Gloudemans et al. (2008) to interpret SCIAMACHY data. The approach is discussed in detail by Borsdorff et al. (2014) and this section summarises its main characteristics. Basically, the retrieval approach scales an n dimensional reference profile ρ_{ref} , which is the input to a radiative transfer model, to fit SCIAMACHY reflectance measurements. Subsequently, we estimate the retrieved CO vertical column density c by

$$c = \mathbf{C}^T \alpha \rho_{\text{ref}}, \quad (1)$$

with the profile scaling factor α . Here, the n dimensional vector $\mathbf{C} = (f_1, \dots, f_n)$ approximates the vertical integration, where f_k converts the k th element of the state vector to the corresponding partial column amount of the trace gas. For sake of simplicity, we refer to the retrieval of the total column density c when meaning this approach in the following.

For the inversion, a forward model F is needed, which describes the m dimensional measurement \mathbf{y}_{meas} within the spectral error \mathbf{e}_y , namely

$$\mathbf{y}_{\text{meas}} = F(\mathbf{x}, \mathbf{b}) + \mathbf{e}_y. \quad (2)$$

Here, state vector \mathbf{x} contains all parameters to be retrieved including the column density of CO and other trace gases. The forward model vector \mathbf{b} includes all parameters which are needed for the simulation but are assumed to be known a priori. For

Title Page

Abstract

Introduction

Conclusions

References

Tables

Figures

◀

▶

◀

▶

Back

Close

Full Screen / Esc

Printer-friendly Version

Interactive Discussion



SCIAMACHY CO total column measurements (2003–2012)

T. Borsdorff et al.

[Title Page](#)

[Abstract](#)

[Introduction](#)

[Conclusions](#)

[References](#)

[Tables](#)

[Figures](#)

[◀](#)

[▶](#)

[◀](#)
[▶](#)

[Back](#)
[Close](#)

[Full Screen / Esc](#)

[Printer-friendly Version](#)

[Interactive Discussion](#)



the measurement, we employ a non-scattering radiative transfer model (Vidot et al., 2012) which simulates atmospheric transmission including Lambertian reflection at the Earth surface. Figure 1 shows a typical transmission spectrum in the retrieval window for clear-sky conditions and the individual spectral contributions of the trace gases HDO, CO, H₂O and CH₄. The forward model employs the cross section database by Gloudemans et al. (2009), which comprises CO and CH₄ absorption cross sections from Rothman et al. (2005) and Predoi-Cross et al. (2006), respectively, and H₂O and HDO cross sections from Jenouvrier et al. (2007). The spectral fit window is extended significantly with respect to the window used by Gloudemans et al. (2008) to establish a stable retrieval for the entire mission period. This is particularly important for the later years of the mission with a significant loss of spectral pixels of the SCIAMACHY channel 8 detector due to radiation damage. The selected window includes strong absorption lines of CH₄ between 2315–2320 nm and a nearly translucent range in the range 2310–2315 nm. Both spectral features are needed to mitigate the degradation of the instrument by fitting effective instrument parameters as described in the following section.

To invert Eq. (2), we employ a Gauss–Newton iteration scheme where the forward model F is linearised each iteration step around the solution x_0 of the previous iteration. Thus, we can rewrite Eq. (2) as

$$y = Kx + e_y \quad (3)$$

with $y = y_{\text{meas}} - F(x_0) + Kx_0$ and the Jacobian or kernel matrix $K = \partial F / \partial x(x_0)$. Subsequently, Eq. (2) is inverted by minimizing the least squares cost function

$$x_{\text{ret}} = \min_x \left\{ \|S_y^{-1/2} (Kx - y)\|_2^2 \right\}, \quad (4)$$

where $\|\cdot\|_2$ represents the L_2 norm and $S_y \in \mathbb{R}^{m \times m}$ is the non-singular measurement error covariance matrix. Simultaneously with CO, we retrieve the vertical column densities of HDO, H₂O, and CH₄ from the SWIR measurements using per species the explained profile scaling approach. Additionally, we infer a wavelength dependent albedo

described by a quadratic polynomial with respect to wavelength. The solution of Eq. (4) can be expressed by the gain matrix \mathbf{G} ,

$$\mathbf{x}_{\text{ret}} = \mathbf{G}\mathbf{y} \quad (5)$$

with

$$\mathbf{G} = (\mathbf{K}^T \mathbf{S}_y^{-1} \mathbf{K})^{-1} \mathbf{K}^T \mathbf{S}_y^{-1}. \quad (6)$$

The retrieved vertical column density c_{ret} is an effective column product due to the regularisation inherent to the profile scaling approach. The relation between the effective column and the true atmospheric abundance is described by the total column averaging kernel \mathbf{a}_{col}

$$C_{\text{ret}} = \mathbf{a}_{\text{col}} \rho_{\text{true}} + e_c, \quad (7)$$

where e_c is the column retrieval error due to the measurement error e_y and ρ_{true} is the true trace gas profile. A numerically efficient algorithm to calculate \mathbf{a}_{col} is presented in Borsdorff et al. (2014). The total column averaging kernel represents an altitude weighted integration of the true profile taking into account the particular retrieval sensitivity.

The differences between the true column, $c_{\text{true}} = \mathbf{C}^T \rho_{\text{true}}$, and the effective column, $c_{\text{eff}} = \mathbf{a}_{\text{col}} \rho_{\text{true}}$, cannot be inferred from the measurement and is also known as the null space or smoothing error of the retrieval (Borsdorff et al., 2014; Rodgers, 2000),

$$e_{\text{null}} = (\mathbf{C}^T - \mathbf{a}_{\text{col}}) \rho_{\text{true}}. \quad (8)$$

Finally, we characterise the noise on the retrieval product due to the measurement noise, described by the retrieval noise covariance

$$\mathbf{S}_x = \mathbf{G} \mathbf{S}_y \mathbf{G}^T. \quad (9)$$

In this manner, we have defined all diagnostic tools for our retrieval. A detailed overview of the profile-scaling approach is given in Borsdorff et al. (2014).

SCIAMACHY CO total column measurements (2003–2012)

T. Borsdorff et al.

[Title Page](#)

[Abstract](#)

[Introduction](#)

[Conclusions](#)

[References](#)

[Tables](#)

[Figures](#)

◀

▶

[Back](#)

[Close](#)

[Full Screen / Esc](#)

[Printer-friendly Version](#)

[Interactive Discussion](#)



The retrieval depends on a priori information, which is adopted from different sources. Surface pressure, temperature profiles and water vapor reference profiles (H_2O , HDO) are based on the ECMWF Re-Analysis Interim (ERA-Interim) data set, which is sampled every 6 h on 60 vertical layers and on a 0.75° latitude by 0.75° longitude grid (Dee et al., 2011). CO and CH_4 -reference profiles are taken from simulations of the 3-dimensional global chemistry transport model TM5 for the period 2003–2012 (Williams et al., 2013, 2014). Atmospheric trace gas profiles are provided every 3 h on 34 layers and on a 2° latitude by 3° longitude grid. For every SCIAMACHY measurement, the model data are spatially resampled to the satellite ground pixel. Moreover, we account for the differences between the mean SCIAMACHY pixel elevation and the mean pixel elevation of the model data. First, we calculate the mean SCIAMACHY pixel height using the digital Shuttle Radar Topography Mission (SRTM) elevation map with a spatial resolution of 15 arc seconds (Farr et al., 2007) and subsequently, all model profiles are interpolated to the mean altitude of a SCIAMACHY ground pixel.

One may question the relevance of the null-space error and the need for column averaging kernels for a proper validation of our data product. Generally, the correct use of Eq. (7) requires measurements of the CO vertical profile. However, this hampers any validation of the SCIAMACHY CO data product because measurements of CO profiles are hardly available for the mission period. On the other hand, a direct comparison of ground based measurements of the total CO column with our data product suffers from the null-space error. Borsdorff et al. (2014) showed from simulations that in the presence of clouds the null space error can easily exceed 30 % of the CO total column. The error is much smaller for clear sky conditions, depending on the reference profile used for scaling. To estimate the null-space error, we consider simulated retrievals for a set of solar zenith angles between 20 and 70° . Here, we used the US standard atmosphere (NOAA, 1976) for the profiles of dry air density, pressure, water and CO. The CH_4 -profile is adopted from the CAMELOT European background model atmosphere (Levelt et al., 2009). The total column averaging kernels are shown in the left panel of Fig. 2. Subsequently, we investigate the null-space error due to the difference of

SCIAMACHY CO total column measurements (2003–2012)

T. Borsdorff et al.

[Title Page](#)

[Abstract](#)

[Introduction](#)

[Conclusions](#)

[References](#)

[Tables](#)

[Figures](#)

◀

▶

[Back](#)

[Close](#)

[Full Screen / Esc](#)

[Printer-friendly Version](#)

[Interactive Discussion](#)



Title Page	
Abstract	Introduction
Conclusions	References
Tables	Figures
◀	▶
◀	▶
Back	Close
Full Screen / Esc	
Printer-friendly Version	
Interactive Discussion	

5 533 CO profiles measured by the HIAPER Pole-to-Pole Observations (HIPPO) of the Carbon Cycle and Greenhouse Gases Study (Wofsy, 2011; Wofsy et al., 2012) and two different choices for the reference profiles. First, we consider the CO US standard profile and second we make use of the collocated CO profiles from the TM5 chemical
transport model, which is the baseline of our algorithm. After scaling to the same total
column, the variation of the HIPPO profiles and the corresponding reference profiles,
are shown in the middle panel of Fig. 2. Finally, the right panel of the figure shows the
corresponding distribution of the null-space error utilising the column averaging kernels
of the same figure. For both cases, the null space error is less than 1 ppb (< 1 %
10 of a mean CO total column) and so far less than the SCIAMACHY measurement noise
error that varies between 30 ppb and > 170 ppb for individual retrievals (see Figs. 6a
and 7a). This means that within an accuracy < 1 % for clear sky SCIAMACHY CO re-
trievals the null space error can be ignored. So a direct comparison between ground
based measurements and SCIAMACHY retrievals is possible. Following this approach,
15 strict cloud filtering of SCIAMACHY data is required. For this purpose, we employ the
SCIAMACHY polarisation device (PMD) Identification of Clouds and Ice (SPICI) algo-
rithm (Krijger et al., 2005).

3 Instrument calibration

In this section, we consider SCIAMACHY nadir measurements for the full operational
20 phase of the mission from January 2003 to April 2012, where we use Level 1b spectra
disseminated by ESA. The measurements are corrected for memory-nonlinearity and
dark current using the Netherlands SCIAMACHY Data Center (NADC) toolbox Version
1.2 (<http://www.sron.nl/~richardh/>). Data recorded during SCIAMACHY's commission-
ing phase are not considered. The CO data processing relies on SCIAMACHY's for-
ward scans for a solar zenith angle smaller than 80° and with a ground pixel size of
25 about 30 km × 120 km (along-track × a cross track) for an integration time of 0.5 s. At

higher northern and southern latitudes the integration time is increased to 1 s, which accordingly doubles the a cross track pixel size.

The SCIAMACHY detector in the 2.3–2.4 μm range (channel 8) suffers from detector radiation damage and very noisy detector pixels. Buchwitz et al. (2007); Gloudemans et al. (2008) showed the severe sensitivity of CO retrievals to the instrument malfunction. A stable retrieval performance for the entire mission lifetime requires careful and strict spectral filtering of bad detector pixels based on in-flight detector performance monitoring. For measurements after 11 January, 2005, we utilise the NADC version 3.0 time-dependent pixel mask and for earlier measurements, we fixed the pixel mask to that of this reference date. The channel 8 SCIAMACHY measurement noise is dominated by detector dark noise, which is estimated from SCIAMACHY's daily dark state measurements taken during the orbit eclipse.

Despite the strict filtering, the absolute radiometric calibration of SCIAMACHY Earth-shine measurements is not accurate enough to retrieve CO. Figure 3 shows the time dependence of the mean solar signal. Besides the seasonal variation of the signal due to the change of the Earth–Sun distance through out the year, the effect of the ice layer formation on the overall instrument transmission and the signal recovery due to the instrument heating during so-called decontamination events (see Table 1) is clearly visible (Gloudemans et al., 2005). To mitigate effects on the CO data quality, our retrieval is based on the reflectance r_i , which is the ratio of the Earth radiance measurement I_i divided by the solar measurement S_i by the same detector pixel i , $r_i = I_i/S_i$. Here, we use SCIAMACHY's daily Sun mean reference measurements, determined from the Sun measurements via the elevation scan mirror. Subsequently, the solar measurements are interpolated to the measurement time of the Earthshine observation to account for a rapidly changing instrument directly after a thermal decontamination event.

The approach implies that any common multiplicative radiometric error of the Earth and solar observations cancels out in the reflectance ratio. However, any additive error component, e.g. due to detector hysteresis, non-linear radiometric detector response, dark detector current and analog offset, still affects the radiometric accuracy of the

Title Page

Abstract

Introduction

Conclusions

References

Tables

Figures

◀

▶

◀
Back▶
Close

Full Screen / Esc

Printer-friendly Version

Interactive Discussion



reflectance spectrum and has to be accounted for by the radiometric calibration procedure.

Moreover, the use of SCIAMACHY reflectance measurements is hampered by the different malfunctioning pixels of the SCIAMACHY channel 8 detector for the Earth-shine and solar observation mode. Filtering on both types of detector performance results in insufficient spectral coverage. To overcome this problem, we identify outliers in the solar irradiance spectrum and replace them by interpolated values. We start with a solar reference measurement $S(t_0, i)$ from 11 January 2003 (Fig. 4, upper panel), which is representative for a well performing nearly ice-free detector (see Fig. 3). The nearly linear dependence of the solar signal on wavelength is due to the spectral variation of the detector pixel quantum efficiency. To detect spectral outliers, we determine the relative difference of the spectrum with respect to its running median spectrum, assuming an average over 1.4 nm. Difference between the original and spectrally smoothed solar spectrum of $> 7\%$ are classified as outliers and are replaced by the smoothed value of the running median spectrum. Smaller differences are attributed to the pixel-to-pixel gain variation of the detector and the measurement noise and these features are maintained in the spectrum. This approach is based on the assumption that spectral variations in the solar spectrum in the considered spectral range are smooth.

In the following, we assume that the degradation of the solar spectrum can be described by

$$S_i(t) = \alpha(t) \cdot \beta_i(t) \cdot S_i(t_0) + \epsilon_i(t), \quad (10)$$

where α describes the relative degradation of the mean signal shown in Fig. 3, β represents the relative spectral degradation of detector pixel i and ϵ_i summarises high frequency error contributions including noise and outliers. The middle panel of Fig. 4 shows the ratio $S_i(t)/(\alpha(t)S_i(t_0))$ for three exemplary days in the year 2003. Applying 1.0 nm running median suppresses high frequency contributions and by that allows us to estimate the degradation function β from the data. Subsequently, this defines also

Title Page

Abstract

Introduction

Conclusions

References

Tables

Figures

◀

▶

◀
Back▶
Close

Full Screen / Esc

Printer-friendly Version

Interactive Discussion



Title Page	
Abstract	Introduction
Conclusions	References
Tables	Figures
	
Back	Close
Full Screen / Esc	
Printer-friendly Version	
Interactive Discussion	

the error contribution $\epsilon_i(t)$ in Eq. (10), which can be used to detect spectral outliers in the solar measurement $S_i(t)$. Any measurement with $\epsilon_i(t) > 2\%$ is classified as outlier and is replaced by the expected value $a(t)\beta_i(t)S_i(t_0)$. In summary, the approach allows to replace corrupted signals by interpolated values assuming a spectrally smooth degradation. High frequency pixel-to-pixel variation present in the reference spectrum $S(t_0)$ are considered to be constant over the entire mission lifetime.

To account for an imperfect calibration resulting in an additive radiometric bias, we consider the Sahara region between 30 and 15° northern latitude and –15 and 30° longitude as a natural calibration target for the entire mission period. This region is chosen because of the high signal levels due to the high reflective desert surface, and because it is assured that the amount of CH₄ can be relatively well predicted using the TM5 model (Gloudemans et al., 2005). For measurements over this particular region, we modify our forward model by adding a polynomial expansion of an additive radiometric bias,

$$F(\mathbf{x}, \mathbf{b}, \mathbf{a}) = \hat{F}(\mathbf{x}, \mathbf{b}) + \sum_{i=0}^3 a_i \cdot p_i(\lambda) \quad (11)$$

Here, $\hat{F}(\mathbf{x}, \mathbf{b})$ denotes the forward calculation in Eq. (2), p_i are Chebyshev polynomials as function of wavelength λ . The coefficients a_i can be determined as additional fit parameters of the retrieval algorithm because of the high radiometric signal over the desert region, where we fix the atmospheric methane abundance to the a priori model information. To fully exploit this approach, it was necessary to include the strong CH₄ absorption between 2315–2320 nm in our spectral fitting window (see Fig. 1).

Figure 5 shows the temporal evolution of coefficient a_0 , which represents a spectrally constant additive bias of the measurement. Here a_0 increases with a growing ice layer while the overall optical throughput of the instrument declines (see Fig. 3). For a fully established ice layer, the offset is 20–30 %. We attribute this offset to photons scattered in the ice layer and then detected at a spectrally shifted position on the detector. In other words, the effective spectral instrument response function is altered

Title Page	
Abstract	Introduction
Conclusions	References
Tables	Figures
	
◀	▶
Back	Close
Full Screen / Esc	
Printer-friendly Version	
Interactive Discussion	

by the ice layer (Gloudemans et al., 2005). To account for this significant bias in our overall retrieval, we smooth the data over a 40 day period and correct all SCIAMACHY measurements accordingly. To demonstrate the general applicability of our approach to global datasets, we applied the same procedure for corresponding cloud free measurements over Australia with a lower surface albedo and with different solar geometries.
 5 We obtained very similar radiometric biases (see Fig. 5) which supports the overall validity of the approach.

Subsequently, we evaluate the spectral calibration and the SCIAMACHY instrument spectral response function. Based on gas-cell measurements during the on-ground calibration of the instrument, Schrijver (1999, 2000b, 2001b) suggested to use a quadratic polynomial in pixel number for the wavelength calibration for the channel 8 detector,
 10

$$\lambda = a_0 + a_1 \cdot n + a_2 \cdot n^2, \quad (12)$$

where wavelength λ is given in nm and n denotes the spectral pixel number. For the purpose of this study, we adopt coefficient $a_1 = 0.135254$ nm and $a_2 = -1.19719 \times 10^{-5}$ nm from the previous studies but reevaluated coefficient a_0 using the Sahara calibration scenes giving $a_0 = 2259.24$ nm.
 15

Finally, we utilise the instrument spectral response function s as determined from pre-flight line source measurements (Schrijver, 2000a, 2001a),

$$s(n, n_0) = \frac{1}{N} \cdot \left(b_0 \cdot \frac{b_1^2}{b_1^2 + (n - n_0)^2} + (1 - b_0) \cdot \frac{b_1^2}{b_1^2 + (n - n_0)^4} \right) \quad (13)$$

20 with $b_0 = 0.7532$, $b_1 = 0.4313$. N controls the overall normalisation of the response function and n denotes the pixel number, where n_0 represents the center pixel. Substitution of Eq. (12) in Eq. (13) allows us to adjust the full width half maximum (FWHM) of the response function for the Sahara calibration scenes. Here, the FWHM varies between 0.19 and 0.24 nm which correlates with the growth of the detector ice-layer (not shown). However, since the effect on the CO retrieval was minor, we fixed the FWHM to a representative value of 0.21 nm.
 25

4 Validation

To validate our SCIAMACHY CO data product, we have to treat two main problems: First the retrieved CO column suffers severely from measurement noise. The retrieval noise error for low radiance signal can exceed 100 % of the retrieved column. Therefore, any validation can only be performed on quantities averaged in space and time. Second, a direct comparison with ground based measurements is affected by representation errors. For example, a monthly mean CO concentration derived from ground based measurements may differ from a corresponding monthly mean of SCIAMACHY measurements due to different temporal sampling. A strict temporal co-registration criterion for both ground based and SCIAMACHY measurements may reduce the sampling effect but at the cost of less SCIAMACHY samplings, which in turn enhances the noise contribution. Both aspects have to be considered in an appropriate validation strategy of the SCIAMACHY CO data product.

4.1 Ground based Fourier Transform Spectrometers

In this section, we validate the SCIAMACHY CO data product with the measurements of Fourier Transform Spectrometers used for observing CO column densities under clear-sky conditions allowing direct Sun measurements. Table 2 summarises the validation dataset, which comprises measurements at various stations of the Infrared Working Group (IRWG) that is part of the Network for the Detection of Atmospheric Composition Change (NDACC, <http://www.ndsc.ncep.noaa.gov/>) and of the Total Carbon Column Observing Network (TCCON) (Wunch et al., 2010, 2011). The IRWG provides measurements in the mid-infrared with the aim to analyse the atmospheric composition of the troposphere and stratosphere. The NDACC-IRWG supplies CO total columns that we transformed to column mixing ratios by calculating air columns from the surface pressures at a station. At several sites, the data record covers the entire SCIAMACHY lifetime and, thus, makes these dataset very suited for the validation of the SCIAMACHY data product. The TCCON network collects measurements

AMTD

8, 9731–9783, 2015

SCIAMACHY CO total column measurements (2003–2012)

T. Borsdorff et al.

Title Page

Abstract

Introduction

Conclusions

References

Tables

Figures

◀

▶

◀
Back

▶
Close

Full Screen / Esc

Printer-friendly Version

Interactive Discussion



in the same spectral range as recorded by SCIAMACHY from space. This results in a similar vertical sensitivity of both the SCIAMACHY and the TCCON product, which is in particular desirable for validation purposes (see e.g. Wunch et al., 2010, Fig. 3 and Borsdorff et al., 2014, Fig. 2). In 2004, TCCON started with the first instrument at Park Falls, US, and since then the network has grown gradually to 19 observation sites worldwide. Therefore, the TCCON dataset is very well suited to validate SCIAMACHY measurements in the later years of the mission. This study is based on the TCCON GGG2014 dataset (Deutscher et al., 2014; Wennberg et al., 2014c, e, a, b, d; Griffith et al., 2014a, b; Strong et al., 2014; Sussmann and Rettinger, 2014; Blumenstock et al., 2014; Kawakami et al., 2014; Sherlock et al., 2014; Warneke et al., 2014; Maziere et al., 2014; Kivi et al., 2014; Morino et al., 2014). Measurements at Ny-Alesund, Bremen, and Four Corners are taken from the GGG2012 data set since those are not yet available in the 2014 data release.

To achieve the best quality of the SCIAMACHY data, we apply an a posteriori quality filter based on the following criteria:

1. The spectral fit residual χ^2 must be < 10 .
2. The mean signal-to-noise ratio of the measurements in the fit window must be > 10 .
3. The noise ϵ of the retrieved CO, CH₄ and H₂O column must be below an upper threshold, namely $\epsilon_{\text{CO}} < 1 \times 10^{19}$, $\epsilon_{\text{CH}_4} < 6 \times 10^{18}$, $\epsilon_{\text{H}_2\text{O}} < 2 \times 10^{22} \text{ molec cm}^{-2}$.
4. Only SCIAMACHY measurements are used, which are classified as cloud free by the SPICI algorithm.

Moreover, we selected SCIAMACHY measurements over land, which fall within a radius of 850 km around a TCCON or NDACC-IRWG station site. To derive one representative monthly value for both datasets, we interpolate the FTIR measurements to the point of the SCIAMACHY measurements at time t . For this purpose, we consider the ratio of the FTIR columns divided by the co-aligned TM5 columns at two adjacent

[Title Page](#)[Abstract](#)[Introduction](#)[Conclusions](#)[References](#)[Tables](#)[Figures](#)[◀](#)[▶](#)[◀](#)[▶](#)[Back](#)[Close](#)[Full Screen / Esc](#)[Printer-friendly Version](#)[Interactive Discussion](#)

FTIR samples, $\delta(t_1)$ and $\delta(t_2)$ at time t_1 and t_2 . The temporal interpolated FTIR column $c^{\text{FTIR}}(t)$ is then given by

$$c^{\text{FTIR}}(t) = \delta(t) \cdot c^{\text{TM5}}(t) \quad (14)$$

where $c^{\text{TM5}}(t)$ is the corresponding TM5 CO column and $\delta(t)$ is the linear function through the adjacent points $\delta(t_1)$ and $\delta(t_2)$. Beforehand, we applied an additive bias correction to the TM5 model values such that the overall mean of the FTIR and TM5 values are the same. This simple interpolation scheme makes use of the precise FTIR measurement where the relative temporal trend in CO due to meteorology and photochemistry is adopted from the TM5 model. Subsequently, we correct $c^{\text{FTIR}}(t)$ for differences between the surface elevation at the station site and the mean altitude of the individual satellite ground pixels using also TM5 CO profiles.

In this manner, we obtain two coaligned datasets, which are subsequently used to derive monthly median CO column concentrations. The scattering of the individual SCIAMACHY retrievals, which underlies each monthly median, is described by the half difference of the 15.9th and the 84.1th percentile e_S to be an analogue for the standard deviation of a normal distribution. For the same SCIAMACHY retrievals, we also calculate the mean retrieval noise e_N . To characterise the retrieval performance per station, we determine the bias b as the mean difference between the monthly median CO concentrations of the ground based and SCIAMACHY retrievals. Moreover, we use the standard deviations σ of these difference and the standard error of the mean s_e to characterise the accuracy of b . Finally to characterise the overall performance, we determine the global mean bias \bar{b} as the mean of the individual station biases weighted by their standard error s_e and the corresponding mean standard deviation $\bar{\sigma}$ and the mean standard error \bar{s}_e .

For all NDACC and TCCON station in Table 2, Figs. 6a and 7a show time series of CO monthly median columns, where Fig. 8 summarises the validation diagnostics. Overall, the larger scatter of the individual SCIAMACHY CO columns is mainly caused by the large measurement noise indicated by the similar values of e_S and e_N . For some

[Title Page](#)[Abstract](#)[Introduction](#)[Conclusions](#)[References](#)[Tables](#)[Figures](#)[◀](#)[▶](#)[◀](#)[▶](#)[Back](#)[Close](#)[Full Screen / Esc](#)[Printer-friendly Version](#)[Interactive Discussion](#)

stations, e_N even exceeds a typical mean CO concentration indicating the need to average data for validation purposes. For the sites Eureka, Ny-Alesund, Sodankyla, Thule, Kiruna, Herestua, Mauna Loa, Reunion, Tsukuba, Saga, and Lauder the noise in the data is even so large that monthly median values are still dominated by measurement noise. For the remaining stations, the scatter of the monthly median is reasonable, and for stations with a mean instrumental noise error $\bar{e}_N < 60$ ppb, the seasonal CO cycle becomes clearly visible in the SCIAMACHY time series. The high noise variability can be explained by a corresponding change of the mean signal strength because of varying surface albedo and solar zenith angle, both governing the amount of solar light reflected at the Earth surface.

Overall, Fig. 8 shows a good agreement between SCIAMACHY and TCCON ground based measurements with a global bias of -1.2 ± 7.2 ppb. For some stations, we observe higher bias, e.g. at Reunion $b = 39$ ppb. These biases come along with large standard error due to a small number of measurements indicating a large uncertainty of b (see Fig. 7a). For the NDACC-IRWG sites, we find a negative global bias $\bar{b} = -9.2 \pm 8.1$ ppb of the SCIAMACHY CO retrieval with respect to the NDACC-IRWG observations. Here, biases for mountain stations like Zugspitze, Jungfraujoch and Izana differ significantly from those at other sites. For the mountain sites, our correction for altitude differences between validation site and the SCIAMACHY ground pixel exceeds 50 % of the CO column and by that our validation is dominated by uncertainties of the TM5 model. The different global biases for TCCON and NDACC-IRWG measurements can be partly explained by the different temporal sampling of the validation sets combined with a small but significant trend of $\bar{t} = 1.47 \pm 0.25$ ppb yr $^{-1}$ in the SCIAMACHY CO columns. Figure 9 resolves this trend for 7 NDACC-IRWG and TCCON stations, which cover the full SCIAMACHY mission period combined with low retrieval noise. The average trend \bar{t} is calculated by a average of the individual trends weighted by their uncertainty, where we excluded measurements at Toronto because of a discontinuity of the NDACC-IRWG time series (see Fig. 6a). This issue is already under investigation and does appear to be instrumental. When correcting the SCIAMACHY data for

SCIAMACHY CO total column measurements (2003–2012)

T. Borsdorff et al.

[Title Page](#)

[Abstract](#)

[Introduction](#)

[Conclusions](#)

[References](#)

[Tables](#)

[Figures](#)

◀

▶

[Back](#)

[Close](#)

[Full Screen / Esc](#)

[Printer-friendly Version](#)

[Interactive Discussion](#)



this trend, the bias with NDACC-IRWG becomes -8.4 ppb and with TCCON -4.6 ppb. Hence, a difference of 3.8 ppb remains between the TCCON and NDACC-IRWG validation. We consider this difference to be significant due to the small mean standard error \bar{s}_e and we conclude that it is most probably caused by a discrepancy between the
5 TCCON and NDACC-IRWG retrievals. This is further confirmed by direct comparison of TCCON and NDACC-IRWG measurements performed at the same station.

4.2 MOZAIC/AGOS aircraft measurements

Additionally, we validate the SCIAMACHY CO data product with CO total columns that are calculated from aircraft CO profile measurements supplied within the
10 MOZAIC/AGOS project. Since 1994, regular profile measurements of reactive gases by several long-distance passenger airliners were performed during ascent and descent phases (in total more than 40,000 flights). Nédélec et al. (2003) indicated that total columns can be derived from those profile measurements with a precision of about $\pm 5\%$. Table 3 summarises the validation dataset, which comprises CO profile measurement at 26 airports worldwide. At many airports the dataset covers the early years
15 of the SCIAMACHY mission and by that forms a complement to the TCCON dataset used in the previous section. More information about the MOZAIC/AGOS program and its data products is provided by Marenco et al. (1998) and Nédélec et al. (2015) and can be found at <http://www.iagos.org/>.

For the comparison with the SCIAMACHY CO retrieval, we only select
20 MOZAIC/AGOS profiles that reach at least 300 hPa and have measurements in every 100 hPa altitude bin. Above the maximum flight altitude, the profiles are extended using the Monitoring Atmospheric Composition and Climate (MACC) reanalysis data at 12:00 UTC. MACC is pre-operational Copernicus Atmosphere Service, which provides
25 data records of CO and other atmospheric trace gases (Ozone, Nitrogen Oxides) as well as aerosols and is covering the 10 years from 2003 to 2012 (Inness et al., 2013, 2015). The derived CO profiles are vertically integrated to obtain an estimate of the CO total columns. For comparison, individual SCIAMACHY retrievals are quality fil-

[Title Page](#)[Abstract](#)[Introduction](#)[Conclusions](#)[References](#)[Tables](#)[Figures](#)[◀](#)[▶](#)[◀](#)
[Back](#)[▶](#)
[Close](#)[Full Screen / Esc](#)[Printer-friendly Version](#)[Interactive Discussion](#)

tered a posteriori as described in Sect. 4.1. Because the MOZAIC/AGOS dataset is temporally more sparse than the ground-based FTIR dataset in Sect. 4.1, we apply a slightly different collocation approach, proposed by de Laat et al. (2012). Here, SCIAMACHY CO columns are spatially averaged within a $8^\circ \times 8^\circ$ ($\pm 4^\circ$) area surrounding an airport location. Temporal averages are calculated around each MOZAIC/AGOS sample, where the time window of averaging is chosen such that the retrieval noise of the average is equal or smaller than 10^{17} molecules cm^{-2} (3.7 ppb). This yields a nonuniform sampling in time with samples of comparable retrieval noise.

Figure 10a shows time series of collocated SCIAMACHY and MOZAIC/AGOS CO total columns for 26 airport locations with more than 13 collocations (similar to Figs. 6a and 7a). Overall, the agreement between both datasets is good. Part of the data scatter is related to the spatio-temporal variability in CO. This affects both datasets differently, where SCIAMACHY samples represent an average for a larger area surrounding the airport, and MOZAIC/AGOS columns are derived from slant profiles measured during descend and ascent of the aircraft over horizontal differences of 200–400 km. The good agreement of both datasets in their seasonal cycle is noticeable for Windhoek airport. Here, CO is subject to a strong seasonal cycle due to biomass burning and the high surface albedo permits SCIAMACHY CO retrieval with a low instrument noise error. For airports like Beijing and Tehran, we notice high value outliers, where the MOZAIC/AGOS columns are much larger than those measured by SCIAMACHY. This bias can be attributed to representation errors comparing localised pollution with spatial averages of SCIAMACHY CO observations. Overall, our results are in agreement with the findings of de Laat et al. (2012) analysing the SCIAMACHY CO measurements before 2009. Figure 11 summarises the fairly good agreement between SCIAMACHY and MOZAIC/AGOS. We find a global bias of -6.4 ± 5.6 ppb. The difference between SCIAMACHY and MOZAIC/AGOS shows a small but significant positive trend of 1.2 ± 0.7 ppb yr^{-1} , which is in agreement with Sect. 4.1. When correcting the SCIAMACHY data for this trend, the global bias reduces to 2.5 ppb which is in the range of the MOZAIC/AGOS CO column uncertainty as reported by Nédélec et al. (2003).

[Title Page](#)[Abstract](#)[Introduction](#)[Conclusions](#)[References](#)[Tables](#)[Figures](#)[◀](#)[▶](#)[◀](#)
[▶](#)[Back](#)[Close](#)[Full Screen / Esc](#)[Printer-friendly Version](#)[Interactive Discussion](#)

5 Potential data application

One fundamental limitation of the SCIAMACHY CO data product is its large noise contribution. For most applications, individual CO columns must be averaged to reduce the retrieval noise to an acceptable level. The degree of averaging depends the signal-to-noise ratio of the corresponding SCIAMACHY observations and therefore on the brightness of the observed scenes. For example, for regions in Africa and Australia with high surface albedo, the retrieval is much higher than over dark scenes at high Northern latitudes with low solar zenith angle. To mitigate this effect, one can consider dataset which are averaged both spatial and temporally. Averaging over the full-mission period (January 2003–April 2012), we obtain the CO global distribution shown in Fig. 12. It illustrates that a high spatial resolution can be achieved with the SCIAMACHY CO retrievals sacrificing temporal resolution. One of the most striking features of Fig. 12 is the enhanced CO column concentrations over central Africa due to biomass burning. To illustrate the seasonal variation of CO in this region, Fig. 13 shows the 30 days median of the SCIAMACHY CO concentration for Northern Hemispheric Africa (averaged between 0 and 10° latitude) and Southern Hemispheric Africa (averaged between 0 and -35° latitude). The figure also includes corresponding averages of TM5 model simulations which use GFED version 3 for the biomass burning input. Overall, the SCIAMACHY and TM5 fields agree well. The seasonal variation is present in both data sets including the phase shift between the Northern and Southern Hemispheric CO concentration. In this case, the seasonal variation of CO can be resolved with SCIAMACHY but at a cost of a poor spatial sampling. This example illustrates nicely the limitations but also the strength of the presented SCIAMACHY CO data product.

6 Summary and conclusions

We presented a full-mission data set of SCIAMACHY CO vertical column densities for cloud-free scenes over land. The retrieval employs the operational SICOR algorithm

AMTD

8, 9731–9783, 2015

SCIAMACHY CO total column measurements (2003–2012)

T. Borsdorff et al.

Title Page

Abstract

Introduction

Conclusions

References

Tables

Figures

◀

▶

◀
Back

▶
Close

Full Screen / Esc

Printer-friendly Version

Interactive Discussion



SCIAMACHY CO total column measurements (2003–2012)

T. Borsdorff et al.

of the Sentinel-5 Precursor mission and is based on a profile scaling approach using SCIAMACHY 2.3 μm reflectance measurements. For the first time, a stable CO retrieval approach is presented for the entire mission period (January 2003–April 2012), which has to deal with the severe instrument degradation over the nearly 10 years mission period. While previous studies focused on the early years of the SCIAMACHY mission period, we were able to mitigate effects of a changing instrument performance in space on the CO column product. For this purpose, we optimised the retrieval window to account for the serious loss of useful detector pixels caused by radiation damage. Furthermore, we estimated effective instrument parameters, which describe the temporal degradation of SCIAMACHY, using the Sahara region as a natural calibration target. These parameters describe the spectral calibration, a spectral radiometric offset, and the width of the instrument spectral response function. The CO total column amount is inferred simultaneously with methane and water vapor abundances and a Lambertian surface albedo from individual SCIAMACHY measurements assuming a non-scattering model atmosphere.

To obtain atmospheric CO abundances, the retrieval scales a CO reference profile, which represents an specific regularisation of the inversion. Consequently when interpreting the retrieved CO column as an estimate of the true column abundance, the data product suffers from a null space error which describes the error in the inferred trace gas column due to the assumed profile to be scaled. Using 533 HIPPO CO profile measurements, we showed that for clear sky conditions the null-space error is typically $< \pm 1$ ppb. This represents a minor error source and thus is not further considered in the validation of our data product. To ensure clear sky conditions, SCIAMACHY observations are filtered strictly employing the onboard polarisation measurement device of the same instrument (SPICI algorithm).

The full-mission data set is validated with ground-based FTIR measurements at 27 stations of the NDACC-IRWG and TCCON network and MOZAIC/IGAGOS airborne measurements at 26 airports worldwide. Here, measurements of the NDACC-IRWG network cover the entire mission period. TCCON measurements can only be used to

[Title Page](#)[Abstract](#)[Introduction](#)[Conclusions](#)[References](#)[Tables](#)[Figures](#)[◀](#)[▶](#)[Back](#)[Close](#)[Full Screen / Esc](#)[Printer-friendly Version](#)[Interactive Discussion](#)

SCIAMACHY CO total column measurements (2003–2012)

T. Borsdorff et al.

validate the CO product in the later phase of the mission, whereas IAGOS/MOZAIC measurements are mainly available for the early years of the mission. For the validation, it is important to realise the main and principle limitation of the SCIAMACHY CO product, which is its high retrieval noise of individual CO columns. It varies between 5 30 ppb over high albedo scenes and more than 170 ppb over dark ground scenes with low signal to noise measurements. Consequently, averaging of individual data points is essential for practical data usage. Hence, we base our validation on monthly median column abundances for the comparison with the FTIR measurement and instrument error weighted means for the comparison with MOZAIC/IAGOS airborne observations.

10 Overall, we found a good agreement with TCCON measurements with only a global mean bias of $\bar{b} = -1.2$ ppb with a station-to-station bias variation of $\bar{\sigma} = 7.2$ ppb. For NDACC-IRWG network, we obtained a significant mean station bias $\bar{b} = -9.2$ ppb with $\bar{\sigma} = 8.1$ ppb. Moreover for the IAGOS/MOSAIC measurements, we find a mean station bias of $\bar{b} = -6.4$ ppb with $\bar{\sigma} = 5.6$ ppb. We detected a small but significant trend of about $1.47 \pm 0.25 \text{ ppb yr}^{-1}$ in the SCIAMACHY data. Correcting this trend, the bias with the IAGOS/MOSAIC measurements becomes 2.5 ppb, which is within the uncertainty of the IAGOS/MOZAIC measurements. The bias between SCIAMACHY and NDACC-IRWG measurements becomes -8.4 ppb and with the TCCON measurements -4.6 ppb. A discrepancy of 3.8 ppb remains between the global biases with NDACC-15 IRWG and TCCON, which is confirmed by directly comparing NDACC-IRWG and TCCON measurements. There are some possible reasons why the NDACC-IRWG and TCCON retrievals differ in that magnitude. NDACC-IRWG retrievals are done from the 5 μm and TCCON from the same 2.3 μm spectral regions as SCIAMACHY using different retrieval approaches. A disagreement of the line parameters of these regions can 20 easily lead to differences and is under investigation. Further, the retrieval of the two networks are based on different isotopic lines. NDACC-IRWG is using two ^{13}CO and one ^{12}CO line while TCCON retrievals are solely based on ^{12}CO lines. Furthermore, TCCON retrievals are calibrated by scaling the retrieved CO columns to the ones obtained 25 from simultaneous in situ measurements (aircraft sampling or AirCore measurements)

[Title Page](#)[Abstract](#)[Introduction](#)[Conclusions](#)[References](#)[Tables](#)[Figures](#)[◀](#)[▶](#)[Back](#)[Close](#)[Full Screen / Esc](#)[Printer-friendly Version](#)[Interactive Discussion](#)

which is not done with the NDACC-IRWG data. Both ground-based FTIR data sets are very valuable for satellite validation, although for the validation of future satellite mission, like the Sentinel 5 Precursor (S5-P) mission to be launched in 2016, it is desirable to improve the comparability of NDACC-IRWG and TCCON measurements.

Finally to demonstrate potential data use, we showed the seasonal cycle of biomass burning events in central Africa. Averaging the entire mission data set, the biomass burning area can be detected with good spatial resolution. On the other hand, considering monthly median SCIAMACHY CO fields averaged over the Northern and Southern part of central Africa, reflects the spatial and temporal variability of biomass burning events in this region in good agreement with the global chemical transport model TM5.

This study represents the first application of the retrieval algorithm SICOR, which was developed for the operational data processing of the S5-P mission on real measurements of the shortwave infrared spectral range. Using the same retrieval approach for both satellite instruments will ensure the compatibility of the CO data sets of both missions, which is highly desirable from the perspective of longterm atmospheric monitoring. In a follow-up study, we will focus to extend the presented CO data set to SCIAMACHY ocean measurements.

Acknowledgements. SCIAMACHY is a joint project of the German Space Agency DLR and the Dutch Space Agency NSO with contribution of the Belgian Space Agency. The work performed is (partly) financed by NSO and through the SCIAMACHY Quality Working Group (SQWG) by ESA. We acknowledge the European Commission for the support to the MOZAIC project (1994–2003) and the preparatory phase of IAGOS (2005–2012), the partner institutions of the IAGOS Research Infrastructure (FZJ, DLR, MPI, KIT in Germany, CNRS, CNES, Météo-France in France and University of Manchester in UK), ETHER (CNES-CNRS/INSU) for hosting the database, the participating airlines (Lufthansa, Air France, Austrian, China Airlines, Iberia, Cathay Pacific) for the transport free of charge of the MOZAIC/IAGOS instrumentation. MACC data were obtained from <http://www.copernicus-atmosphere.eu>. We acknowledge the NDACC-IRWG and TCCON ground-based FTIR networks for providing data.

AMTD

8, 9731–9783, 2015

SCIAMACHY CO total column measurements (2003–2012)

T. Borsdorff et al.

Title Page

Abstract

Introduction

Conclusions

References

Tables

Figures

◀

▶

Back

Close

Full Screen / Esc

Printer-friendly Version

Interactive Discussion



References

SCIAMACHY CO total column measurements (2003–2012)

T. Borsdorff et al.

Title Page

Abstract

Introduction

Conclusions

References

Tables

Figures

◀

▶

◀

▶

Back

Close

Full Screen / Esc

Printer-friendly Version

Interactive Discussion



SCIAMACHY CO total column measurements (2003–2012)

T. Borsdorff et al.

[Title Page](#)

[Abstract](#)

[Introduction](#)

[Conclusions](#)

[References](#)

[Tables](#)

[Figures](#)

◀

▶

[◀](#)
[Back](#)

[▶](#)
[Close](#)

[Full Screen / Esc](#)

[Printer-friendly Version](#)

[Interactive Discussion](#)



- 5 Farr, T. G., Rosen, P. A., Caro, E., Crippen, R., Duren, R., Hensley, S., Kobrick, M., Paller, M., Rodriguez, E., Roth, L., Seal, D., Shaffer, S., Shimada, J., Umland, J., Werner, M., Oskin, M., Burbank, D., and Alsdorf, D.: The Shuttle Radar Topography Mission, Rev. Geophys., 45, RG2004, doi:10.1029/2005RG000183, 2007. 9739
- Frankenberg, C., Platt, U., and Wagner, T.: Retrieval of CO from SCIAMACHY onboard ENVISAT: detection of strongly polluted areas and seasonal patterns in global CO abundances, Atmos. Chem. Phys., 5, 1639–1644, doi:10.5194/acp-5-1639-2005, 2005. 9734
- 10 Gloudemans, A. M. S., Schrijver, H., Kleipool, Q., van den Broek, M. M. P., Straume, A. G., Lichtenberg, G., van Hees, R. M., Aben, I., and Meirink, J. F.: The impact of SCIAMACHY near-infrared instrument calibration on CH₄ and CO total columns, Atmos. Chem. Phys., 5, 2369–2383, doi:10.5194/acp-5-2369-2005, 2005. 9735, 9741, 9743, 9744
- 15 Gloudemans, A. M. S., Krol, M. C., Meirink, J. F., de Laat, A. T. J., van der Werf, G. R., Schrijver, H., van den Broek, M. M. P., and Aben, I.: Evidence for long-range transport of carbon monoxide in the Southern Hemisphere from SCIAMACHY observations, Geophys. Res. Lett., 33, L16807, doi:10.1029/2006GL026804, 2006. 9733
- 20 Gloudemans, A. M. S., Schrijver, H., Hasekamp, O. P., and Aben, I.: Error analysis for CO and CH₄ total column retrievals from SCIAMACHY 2.3 μm spectra, Atmos. Chem. Phys., 8, 3999–4017, doi:10.5194/acp-8-3999-2008, 2008. 9734, 9736, 9737, 9741
- Gloudemans, A. M. S., de Laat, A. T. J., Schrijver, H., Aben, I., Meirink, J. F., and van der Werf, G. R.: SCIAMACHY CO over land and oceans: 2003–2007 interannual variability, Atmos. Chem. Phys., 9, 3799–3813, doi:10.5194/acp-9-3799-2009, 2009. 9734, 9737
- 25 Griffith, D. W. T., Deutscher, N., Velazco, V. A., Wennberg, P. O., Yavin, Y., Aleks, G. K., Washenfelder, R., Toon, G. C., Blavier, J.-F., Murphy, C., Jones, N., Kettlewell, G., Connor, B., Macatangay, R., Roehl, C., Ryczek, M., Glowacki, J., Culgan, T., and Bryant, G.: TCCON Data from Darwin, Australia, Release GGG2014R0., TCCON data archive, hosted by the Carbon Dioxide Information Analysis Center, Oak Ridge National Laboratory, Oak Ridge, TN, USA, doi:10.14291/tcccon.ggg2014.darwin01.R0/1149290, 2014a. 9746
- 30 Griffith, D. W. T., Velazco, V. A., Deutscher, N., Murphy, C., Jones, N., Wilson, S., Macatangay, R., Kettlewell, G., Buchholz, R. R., and Rigganbach, M.: TCCON Data from Wollongong, Australia, Release GGG2014R0., TCCON data archive, hosted by the Carbon Diox-

SCIAMACHY CO total column measurements (2003–2012)

T. Borsdorff et al.

[Title Page](#)

[Abstract](#)

[Introduction](#)

[Conclusions](#)

[References](#)

[Tables](#)

[Figures](#)

◀

▶

◀

▶

[Back](#)

[Close](#)

[Full Screen / Esc](#)

[Printer-friendly Version](#)

[Interactive Discussion](#)



ide Information Analysis Center, Oak Ridge National Laboratory, Oak Ridge, TN, USA, doi:10.14291/tcccon.ggg2014.wollongong01.R0/1149291, 2014b. 9746

Holloway, T., Levy, H., and Kasibhatla, P.: Global distribution of carbon monoxide, *J. Geophys. Res.*, 105, 12123–12148, doi:10.1029/1999JD901173, 2000. 9733

Inness, A., Baier, F., Benedetti, A., Bouarar, I., Chabriat, S., Clark, H., Clerbaux, C., Coheur, P., Engelen, R. J., Errera, Q., Flemming, J., George, M., Granier, C., Hadji-Lazaro, J., Huijnen, V., Hurtmans, D., Jones, L., Kaiser, J. W., Kapsomenakis, J., Lefever, K., Leitão, J., Razinger, M., Richter, A., Schultz, M. G., Simmons, A. J., Suttie, M., Stein, O., Thépaut, J.-N., Thouret, V., Vrekoussis, M., Zerefos, C., and the MACC team: The MACC reanalysis: an 8 yr data set of atmospheric composition, *Atmos. Chem. Phys.*, 13, 4073–4109, doi:10.5194/acp-13-4073-2013, 2013. 9749

Inness, A., Benedetti, A., Flemming, J., Huijnen, V., Kaiser, J. W., Parrington, M., and Remy, S.: The ENSO signal in atmospheric composition fields: emission-driven versus dynamically induced changes, *Atmos. Chem. Phys.*, 15, 9083–9097, doi:10.5194/acp-15-9083-2015, 2015. 9749

Jenouvrier, A., Daumont, L., Régalias-Jarlot, L., Tyuterev, V. G., Carleer, M., Vandaele, A. C., Mikhailenko, S., and Fally, S.: Fourier transform measurements of water vapor line parameters in the 4200–6600 cm⁻¹ region, *J. Quant. Spectrosc. Ra.*, 105, 326–355, doi:10.1016/j.jqsrt.2006.11.007, 2007. 9737

Kawakami, S., Ohyama, H., Arai, K., Okumura, H., Taura, C., Fukamachi, T., and Sakashita, M.: TCCON Data from Saga, Japan, Release GGG2014R0., TCCON Data Archive, hosted by the Carbon Dioxide Information Analysis Center, Oak Ridge National Laboratory, Oak Ridge, TN, USA, doi:10.14291/tcccon.ggg2014.saga01.R0/1149283, 2014. 9746

Kivi, R., Heikkinen, P., and Kyro, E.: TCCON Data from Sodankyla, Finland, Release GGG2014R0., TCCON Data Archive, hosted by the Carbon Dioxide Information Analysis Center, Oak Ridge National Laboratory, Oak Ridge, TN, USA, doi:10.14291/tcccon.ggg2014.sodankyla01.R0/1149280, 2014. 9746

Krijger, J. M., Aben, I., and Schrijver, H.: Distinction between clouds and ice/snow covered surfaces in the identification of cloud-free observations using SCIAMACHY PMDs, *Atmos. Chem. Phys.*, 5, 2729–2738, doi:10.5194/acp-5-2729-2005, 2005. 9740

Levelt, P. F., Veefkind, J. P., Kerridge, B. J., Siddans, R., de Leeuw, G., Remedios, J., and Coheur, P. F.: Observation Techniques and Mission Concepts for Atmospheric Chemistry

AMTD

8, 9731–9783, 2015

SCIAMACHY CO total column measurements (2003–2012)

T. Borsdorff et al.

[Title Page](#)

[Abstract](#)

[Introduction](#)

[Conclusions](#)

[References](#)

[Tables](#)

[Figures](#)

◀

▶

[Back](#)

[Close](#)

[Full Screen / Esc](#)

[Printer-friendly Version](#)

[Interactive Discussion](#)



(CAMELOT), Report 20533/07NL/HE, European Space Agency, Noordwijk, the Netherlands, 2009. 9739

Logan, J. A., Prather, M. J., Wofsy, S. C., and McElroy, M. B.: Tropospheric chemistry – a global perspective, *J. Geophys. Res.*, 86, 7210–7254, doi:10.1029/JC086iC08p07210, 1981. 9733

5 Marenco, A., Thouret, V., Nédélec, P., Smit, H., Helten, M., Kley, D., Karcher, F., Simon, P., Law, K., Pyle, J., Poschmann, G., von Wrede, R., Hume, C., and Cook, T.: Measurement of ozone and water vapor by Airbus in-service aircraft: the MOZAIC airborne program, an overview, *J. Geophys. Res.*, 103, 25631, doi:10.1029/98JD00977, 1998. 9749

10 Maziere, M. D., Desmet, F., Hermans, C., Scolas, F., Kumps, N., Metzger, J.-M., Duflot, V., and Cammas, J.-P.: TCCON Data from Reunion Island (La Réunion), France, Release GGG2014R0, TCCON Data Archive, hosted by the Carbon Dioxide Information Analysis Center, Oak Ridge National Laboratory, Oak Ridge, TN, USA, doi:10.14291/tccon.ggg2014.reunion01.R0/1149288, 2014. 9746

15 Morino, I., Matsuzaki, T., Ikegami, H., and Shishime, A.: TCCON Data from Tsukuba, Ibaraki, Japan, 125HR, Release GGG2014R0, TCCON Data Archive, hosted by the Carbon Dioxide Information Analysis Center, Oak Ridge National Laboratory, Oak Ridge, TN, USA, doi:10.14291/tccon.ggg2014.tsukuba02.R0/1149301, 2014. 9746

20 Nedelec, P., Cammas, J.-P., Thouret, V., Athier, G., Cousin, J.-M., Legrand, C., Abonnel, C., Lecoeur, F., Cayez, G., and Marizy, C.: An improved infrared carbon monoxide analyser for routine measurements aboard commercial Airbus aircraft: technical validation and first scientific results of the MOZAIC III programme, *Atmos. Chem. Phys.*, 3, 1551–1564, doi:10.5194/acp-3-1551-2003, 2003. 9749, 9750

25 Nédélec, P., Blot, R., Boulanger, D., Athier, G., Cousin, J.-M., Gautron, B., Petzold, A., Volz-Thomas, A., and Thouret, V.: Instrumentation on commercial aircraft for monitoring the atmospheric composition on a global scale: the IAGOS system, technical overview of ozone and carbon monoxide measurements, *Tellus B*, 67, 27791, doi:10.3402/tellusb.v67.27791, 2015. 9749

NOAA: US Standard Atmosphere, 1976, Report NOAA-S/T76-1562, National Oceanic and Atmospheric Administration, Washington, DC, U.S. Gov. Printing Office, 1976. 9739

30 Predoi-Cross, A., Brawley-Tremblay, M., Brown, L. R., Devi, V. M., and Benner, D. C.: Multispectrum analysis of $^{12}\text{CH}_4$ from 4100 to 4635 cm^{-1} : II. Air-broadening coefficients (widths and shifts), *J. Mol. Spectrosc.*, 236, 201–215, doi:10.1016/j.jms.2006.01.013, 2006. 9737

AMTD

8, 9731–9783, 2015

SCIAMACHY CO total column measurements (2003–2012)

T. Borsdorff et al.

[Title Page](#)

[Abstract](#)

[Introduction](#)

[Conclusions](#)

[References](#)

[Tables](#)

[Figures](#)

◀

▶

◀
Back

▶
Close

[Full Screen / Esc](#)

[Printer-friendly Version](#)

[Interactive Discussion](#)



SCIAMACHY CO total column measurements (2003–2012)

T. Borsdorff et al.

[Title Page](#)

[Abstract](#)

[Introduction](#)

[Conclusions](#)

[References](#)

[Tables](#)

[Figures](#)

◀

▶

[Back](#)

[Close](#)

[Full Screen / Esc](#)

[Printer-friendly Version](#)

[Interactive Discussion](#)



Rodgers, C. D.: Inverse Methods for Atmospheric Sounding: Theory and Practice, vol. 2 of Series on Atmospheric, Oceanic and Planetary Physics, World Scientific, Singapore, River Edge, N.J., réimpression: 2004, 2008, 2000. 9738

Rothman, L. S., Jacquemart, D., Barbe, A., Chris Benner, D., Birk, M., Brown, L. R., Carter, M. R., Chackerian, C., Chance, K., Coudert, L. H., Dana, V., Devi, V. M., Flaud, J.-M., Gamache, R. R., Goldman, A., Hartmann, J.-M., Jucks, K. W., Maki, A. G., Mandin, J.-Y., Massie, S. T., Orphal, J., Perrin, A., Rinsland, C. P., Smith, M. A. H., Tennyson, J., Tolchenov, R. N., Toth, R. A., Vander Auwera, J., Varanasi, P., and Wagner, G.: The HITRAN 2004 molecular spectroscopic database, *J. Quant. Spectrosc. Ra.*, 96, 139–204, doi:10.1016/j.jqsrt.2004.10.008, 2005. 9737

Schrijver, H.: Spectral Calibration of SCIAMACHY Channels 7 and 8 Using Gas Cell Absorption Spectra, Tech. Rep. SRON-EOS-HS-99001, issue 1, SRON, Utrecht, the Netherlands, 1999. 9744

Schrijver, H.: Line Profiles for SCIAMACHY Channels 7 and 8 Derived from Gas Cell Absorption Spectra, Tech. Rep. SRON-EOS-HS-00002, issue 1, SRON, Utrecht, the Netherlands, 2000a. 9744

Schrijver, H.: New Spectral Calibration of SCIAMACHY Channels 7 and 8 Using Gas Cell Absorption Spectra, Tech. Rep. SRON-EOS-HS-00001, issue 1, SRON, Utrecht, the Netherlands, 2000b. 9744

Schrijver, H.: Slit Functions for SCIAMACHY Channel 7 and 8, Tech. Rep. SRON-EOS-HS-01001, issue 1, SRON, Utrecht, the Netherlands, 2001a. 9744

Schrijver, H.: Further on Spectral Calibration of SCIAMACHY Channels 7 and 8, Tech. Rep. SRON-EOS-HS-01002, issue 1, SRON, Utrecht, the Netherlands, 2001b. 9744

Seiler, W. and Fishman, J.: The distribution of carbon monoxide and ozone in the free troposphere, *J. Geophys. Res.*, 86, 7255–7265, doi:10.1029/JC086iC08p07255, 1981. 9733

Sherlock, V., Connor, B., Robinson, J., Shiona, H., Smale, D., and Pollard, D.: TCCON Data from Lauder, New Zealand, 120HR, Release GGG2014R0, TCCON Data Archive, hosted by the Carbon Dioxide Information Analysis Center, Oak Ridge National Laboratory, Oak Ridge, TN, USA, doi:10.14291/tcccon.ggg2014.lauder01.R0/1149293, 2014. 9746

Spivakovsky, C. M., Logan, J. A., Montzka, S. A., Balkanski, Y. J., Foreman-Fowler, M., Jones, D. B. A., Horowitz, L. W., Fusco, A. C., Brenninkmeijer, C. A. M., Prather, M. J., Wofsy, S. C., and McElroy, M. B.: Three-dimensional climatological dis-

tribution of tropospheric OH: update and evaluation, *J. Geophys. Res.*, 105, 8931–8980, doi:10.1029/1999JD901006, 2000. 9733

Strong, K., Mendonca, J., Weaver, D., Fogal, P., Drummond, J., Batchelor, R., and Lindenmaier, R.: TCCON Data from Eureka, Canada, Release GGG2014R0, TCCON Data Archive, hosted by the Carbon Dioxide Information Analysis Center, Oak Ridge National Laboratory, Oak Ridge, TN, USA, doi:10.14291/tcccon.ggg2014.eureka01.R0/1149271, 2014. 9746

Sussmann, R. and Rettinger, M.: TCCON Data from Garmisch, Germany, Release GGG2014R0, TCCON Data Archive, hosted by the Carbon Dioxide Information Analysis Center, Oak Ridge National Laboratory, Oak Ridge, TN, USA, doi:10.14291/tcccon.ggg2014.garmisch01.R0/1149299, 2014. 9746

Vidot, J., Landgraf, J., Hasekamp, O., Butz, A., Galli, A., Tol, P., and Aben, I.: Carbon monoxide from shortwave infrared reflectance measurements: a new retrieval approach for clear sky and partially cloudy atmospheres, the Sentinel Missions – new opportunities for science, *Remote Sens. Environ.*, 120, 255–266, 2012. 9734, 9737

Warneke, T., Messerschmidt, J., Notholt, J., Weinzierl, C., Deutscher, N., Petri, C., Grupe, P., Vuillemin, C., Truong, F., Schmidt, M., Ramonet, M., and Parmentier, E.: TCCON Data from Orleans, France, Release GGG2014R0, TCCON Data Archive, hosted by the Carbon Dioxide Information Analysis Center, Oak Ridge National Laboratory, Oak Ridge, TN, USA, doi:10.14291/tcccon.ggg2014.orleans01.R0/1149276, 2014. 9746

Wennberg, P. O., Roehl, C., Blavier, J.-F., Wunch, D., Landeros, J., and Allen, N.: TCCON Data from Jet Propulsion Laboratory, Pasadena, California, USA, Release GGG2014R0, TCCON Data Archive, hosted by the Carbon Dioxide Information Analysis Center, Oak Ridge National Laboratory, Oak Ridge, TN, USA, doi:10.14291/tcccon.ggg2014.jpl02.R0/1149297, 2014a. 9746

Wennberg, P. O., Roehl, C., Wunch, D., Toon, G. C., Blavier, J.-F., Washenfelder, R., Keppel-Aleks, G., Allen, N., and Ayers, J.: TCCON Data from Park Falls, Wisconsin, USA, Release GGG2014R0, TCCON Data Archive, hosted by the Carbon Dioxide Information Analysis Center, Oak Ridge National Laboratory, Oak Ridge, TN, USA, doi:10.14291/tcccon.ggg2014.parkfalls01.R0/1149161, 2014b. 9746

Wennberg, P. O., Wunch, D., Roehl, C., Blavier, J.-F., Toon, G. C., and Allen, N.: TCCON Data from California Institute of Technology, Pasadena, California, USA, Release GGG2014R1, TCCON Data Archive, hosted by the Carbon Dioxide In-

SCIAMACHY CO total column measurements (2003–2012)

T. Borsdorff et al.

[Title Page](#)

[Abstract](#)

[Introduction](#)

[Conclusions](#)

[References](#)

[Tables](#)

[Figures](#)

◀

▶

[Back](#)

[Close](#)

[Full Screen / Esc](#)

[Printer-friendly Version](#)

[Interactive Discussion](#)



SCIAMACHY CO total column measurements (2003–2012)

T. Borsdorff et al.

[Title Page](#)

[Abstract](#)

[Introduction](#)

[Conclusions](#)

[References](#)

[Tables](#)

[Figures](#)

◀

▶

◀
Back

▶
Close

[Full Screen / Esc](#)

[Printer-friendly Version](#)

[Interactive Discussion](#)



formation Analysis Center, Oak Ridge National Laboratory, Oak Ridge, TN, USA, doi:10.14291/tcccon.ggg2014.pasadena01.R1/1182415, 2014c. 9746

Wennberg, P. O., Wunch, D., Roehl, C., Blavier, J.-F., Toon, G. C., Allen, N., Dowell, P., Teske, K., Martin, C., and Martin, J.: TCCON Data from Lamont, Oklahoma, USA, Release GGG2014R0, TCCON Data Archive, hosted by the Carbon Dioxide Information Analysis Center, Oak Ridge National Laboratory, Oak Ridge, TN, USA, doi:10.14291/tcccon.ggg2014.lamont01.R0/1149159, 2014d. 9746

Wennberg, P. O., Wunch, D., Yavin, Y., Toon, G. C., Blavier, J.-F., Allen, N., and Keppel-Aleks, G.: TCCON Data from Jet Propulsion Laboratory, Pasadena, California, USA, Release GGG2014R0, TCCON Data Archive, hosted by the Carbon Dioxide Information Analysis Center, Oak Ridge National Laboratory, Oak Ridge, TN, USA, doi:10.14291/tcccon.ggg2014.jpl01.R0/1149163, 2014e. 9746

Williams, J. E., van Velthoven, P. F. J., and Brenninkmeijer, C. A. M.: Quantifying the uncertainty in simulating global tropospheric composition due to the variability in global emission estimates of Biogenic Volatile Organic Compounds, *Atmos. Chem. Phys.*, 13, 2857–2891, doi:10.5194/acp-13-2857-2013, 2013. 9739

Williams, J. E., Le Bras, G., Kukui, A., Ziereis, H., and Brenninkmeijer, C. A. M.: The impact of the chemical production of methyl nitrate from the NO + CH₃O₂ reaction on the global distributions of alkyl nitrates, nitrogen oxides and tropospheric ozone: a global modelling study, *Atmos. Chem. Phys.*, 14, 2363–2382, doi:10.5194/acp-14-2363-2014, 2014. 9739

Wofsy, S., Daube, B., Jimenez, R., Kort, E., Pittman, J., Park, S., Commane, R., Xiang, B., Santoni, G., Jacob, D., Fisher, J., Pickett-Heaps, C., Wang, H., Wecht, K., Wang, Q.-Q., Stephens, B., Shertz, S., Watt, A., Romashkin, P., Campos, T., Haggerty, J., Cooper, W., Rogers, D., Beaton, S., Hendershot, R., Elkins, J., Fahey, D., Gao, R., Moore, F., Montzka, S., Schwarz, J., Perring, A., Hurst, D., Miller, B., Sweeney, C., Oltmans, S., Nance, D., Hintsa, E., Dutton, G., Watts, L., Spackman, J., Rosenlof, K., Ray, E., Hall, B., Zondlo, M., Diao, M., Keeling, R., Bent, J., Atlas, E., Lueb, R., and Mahoney, M.: HIPPO Merged 10-second Meteorology, Atmospheric Chemistry, Aerosol Data (R_20121129), Carbon Dioxide Information Analysis Center, Oak Ridge National Laboratory, Oak Ridge, TN, USA, doi:10.3334/CDIAC/hippo_010 (Release 20121129), 2012. 9740

Wofsy, S. C.: HIAPER Pole-to-Pole Observations (HIPPO): fine-grained, global-scale measurements of climatically important atmospheric gases and aerosols, *Philos. T. R. Soc. A*, 369, 2073–2086, doi:10.1098/rsta.2010.0313, 2011. 9740

SCIAMACHY CO total column measurements (2003–2012)

T. Borsdorff et al.

[Title Page](#)

[Abstract](#)

[Introduction](#)

[Conclusions](#)

[References](#)

[Tables](#)

[Figures](#)



[Back](#)

[Close](#)

[Full Screen / Esc](#)

[Printer-friendly Version](#)

[Interactive Discussion](#)



Wunch, D., Toon, G. C., Wennberg, P. O., Wofsy, S. C., Stephens, B. B., Fischer, M. L., Uchino, O., Abshire, J. B., Bernath, P., Biraud, S. C., Blavier, J.-F. L., Boone, C., Bowman, K. P., Browell, E. V., Campos, T., Connor, B. J., Daube, B. C., Deutscher, N. M., Diao, M., Elkins, J. W., Gerbig, C., Gottlieb, E., Griffith, D. W. T., Hurst, D. F., Jiménez, R., Keppel-Aleks, G., Kort, E. A., Macatangay, R., Machida, T., Matsueda, H., Moore, F., Morino, I., Park, S., Robinson, J., Roehl, C. M., Sawa, Y., Sherlock, V., Sweeney, C., Tanaka, T., and Zondlo, M. A.: Calibration of the Total Carbon Column Observing Network using aircraft profile data, *Atmos. Meas. Tech.*, 3, 1351–1362, doi:10.5194/amt-3-1351-2010, 2010. 9745, 9746

Wunch, D., Wennberg, P. O., Toon, G. C., Connor, B. J., Fisher, B., Osterman, G. B., Frankenberg, C., Mandrake, L., O'Dell, C., Ahonen, P., Biraud, S. C., Castano, R., Cressie, N., Crisp, D., Deutscher, N. M., Eldering, A., Fisher, M. L., Griffith, D. W. T., Gunson, M., Heikkinen, P., Keppel-Aleks, G., Kyrö, E., Lindenmaier, R., Macatangay, R., Mendonca, J., Messerschmidt, J., Miller, C. E., Morino, I., Notholt, J., Oyafuso, F. A., Rettinger, M., Robinson, J., Roehl, C. M., Salawitch, R. J., Sherlock, V., Strong, K., Sussmann, R., Tanaka, T., Thompson, D. R., Uchino, O., Warneke, T., and Wofsy, S. C.: A method for evaluating bias in global measurements of CO₂ total columns from space, *Atmos. Chem. Phys.*, 11, 12317–12337, doi:10.5194/acp-11-12317-2011, 2011. 9745

Yurganov, L. N., Blumenstock, T., Grechko, E. I., Hase, F., Hyer, E. J., Kasischke, E. S., Koike, M., Kondo, Y., Kramer, I., Leung, F.-Y., Mahieu, E., Mellqvist, J., Notholt, J., Novelli, P. C., Rinsland, C. P., Scheel, H. E., Schulz, A., Strandberg, A., Sussmann, R., Tanimoto, H., Velazco, V., Zander, R., and Zhao, Y.: A quantitative assessment of the 1998 carbon monoxide emission anomaly in the Northern Hemisphere based on total column and surface concentration measurements, *J. Geophys. Res.*, 109, D15305, doi:10.1029/2004JD004559, 2004. 9733

Yurganov, L. N., Duchatelet, P., Dzhola, A. V., Edwards, D. P., Hase, F., Kramer, I., Mahieu, E., Mellqvist, J., Notholt, J., Novelli, P. C., Rockmann, A., Scheel, H. E., Schneider, M., Schulz, A., Strandberg, A., Sussmann, R., Tanimoto, H., Velazco, V., Drummond, J. R., and Gille, J. C.: Increased Northern Hemispheric carbon monoxide burden in the troposphere in 2002 and 2003 detected from the ground and from space, *Atmos. Chem. Phys.*, 5, 563–573, doi:10.5194/acp-5-563-2005, 2005. 9733

SCIAMACHY CO total column measurements (2003–2012)

T. Borsdorff et al.

Table 1. Decontamination events of the SCIAMACHY instrument from 2003–2012. The dates are given together with the corresponding orbit ranges.

number	period	orbits
1	1–4 Jan 2003	4380–4428
2	4–7 Apr 2003	5718–5766
3	21–25 May 2003	6384–6449
4	12–29 Aug 2003	7574–7827
5	18 Dec 2003–5 Jan 2004	9407–9673
6	18–30 Jun 2004	12031–12208
7	20 Dec 2004–5 Jan 2005	14675–14912
8	19 Dec 2008–7 Jan 2009	35574–35848

[Title Page](#)[Abstract](#)[Introduction](#)[Conclusions](#)[References](#)[Tables](#)[Figures](#)[◀](#)[▶](#)[◀](#)[▶](#)[Back](#)[Close](#)[Full Screen / Esc](#)[Printer-friendly Version](#)[Interactive Discussion](#)

Table 2. Ground-based FTIR stations used for validation. The latitude and longitude values are given in degrees, the surface elevation in km, and the overlap in time of the stations (NDACC-IRWG/TCCON) with SCIAMACHY in years.

number	name	lat	lon	alt	NDACC	TCCON
1	Eureka	80.05	-86.42	0.61	2006–2011	2010–2011
2	Ny-Alesund	78.92	11.92	0.02	2003–2011	2005–2011
3	Thule	76.52	-68.77	0.22	2003–2011	–
4	Kiruna	67.84	20.40	0.42	2003–2011	–
5	Sodankyla	67.37	26.63	0.18	–	2009–2011
6	Harestua	60.20	10.80	0.60	2003–2012	–
7	Bialystok	53.23	23.03	0.16	–	2009–2012
8	Bremen	53.10	8.85	0.03	2003–2012	2005–2012
9	Orleans	47.97	2.11	0.13	–	2009–2012
10	Garmisch	47.48	11.06	0.75	2004–2010	2007–2012
11	Zugspitze	47.42	10.98	2.96	2003–2012	–
12	Jungfraujoch	46.55	7.98	3.58	2003–2012	–
13	Parkfalls	45.94	-90.27	0.44	–	2004–2012
14	Toronto	43.66	-79.40	0.17	2003–2012	–
15	Fourcorners	36.80	-108.48	1.64	–	2011–2012
16	Lamont	36.60	-97.49	0.32	–	2008–2012
17	Tsukuba	36.05	140.12	0.03	–	2011–2012
18	JPL	34.13	-118.13	0.21	–	2007–2012
19	Saga	33.24	130.29	0.01	–	2011–2012
20	Kitt Peak	31.90	-111.60	2.09	2003–2005	–
21	Izana	28.30	-16.48	2.37	2003–2012	2007–2012
22	Maunaloa	19.54	-155.57	3.40	2003–2012	–
23	Darwin	-12.43	130.89	0.03	–	2005–2012
24	Reunion	-20.90	55.49	0.09	2004–2011	2011–2012
25	Wollongong	-34.41	150.88	0.03	2003–2008	2008–2012
26	Lauder	-45.05	169.68	0.37	2003–2012	2004–2010
27	Arrivalheights	-77.82	166.65	0.20	2003–2012	–

Title Page

Abstract

Introduction

Conclusions

References

Tables

Figures

◀

▶

◀

▶

Back

Close

Full Screen / Esc

Printer-friendly Version

Interactive Discussion



SCIAMACHY CO total column measurements (2003–2012)

T. Borsdorff et al.

[Title Page](#)

[Abstract](#)

[Introduction](#)

[Conclusions](#)

[References](#)

[Tables](#)

[Figures](#)

◀

▶

◀

▶

[Back](#)

[Close](#)

[Full Screen / Esc](#)

[Printer-friendly Version](#)

[Interactive Discussion](#)

Table 3. Same as Table 2, but for MOZAIC/AGOS airports sites.

number	name	lat	lon	alt	MOZAIC/AGOS
1	London	50.39	0.85	0.03	2006–2009
2	Frankfurt	50.32	7.71	0.11	2003–2011
3	Munich	48.85	12.70	0.45	2003–2011
4	Vienna	48.51	17.36	0.18	2003–2007
5	Portland	46.54	-122.18	0.02	2003–2009
6	Montreal	46.06	-72.65	0.04	2003–2006
7	Toronto	44.46	-78.59	0.17	2003–2011
8	Boston	43.01	-69.95	0.01	2003–2011
9	Chicago	42.79	-86.67	0.20	2003–2010
10	New York	41.23	-72.75	0.00	2003–2006
11	Beijing	40.38	115.22	0.04	2003–2005
12	Philadelphia	40.23	-74.23	0.01	2003–2006
13	Washington	39.94	-76.43	0.10	2004–2012
14	Tehran	35.98	50.24	1.01	2003–2005
15	Los Angeles	34.48	-117.47	0.04	2003–2005
16	Atlanta	34.43	-83.56	0.31	2003–2011
17	Dallas	33.83	-96.04	0.19	2003–2010
18	Tel Aviv	32.77	33.81	0.04	2003–2011
19	Cairo	30.72	31.15	0.12	2003–2011
20	Houston	30.63	-94.26	0.03	2003–2004
21	New Delhi	28.94	76.14	0.24	2003–2006
22	Kuwait City	28.74	48.44	0.06	2003–2004
23	Abu Dhabi	25.90	54.32	0.03	2003–2005
24	Hyderabad	17.54	77.40	0.63	2005–2011
25	Caracas	11.26	-66.37	0.07	2003–2009
26	Windhoek	-21.43	17.34	1.72	2005–2012



SCIAMACHY CO total column measurements (2003–2012)

T. Borsdorff et al.

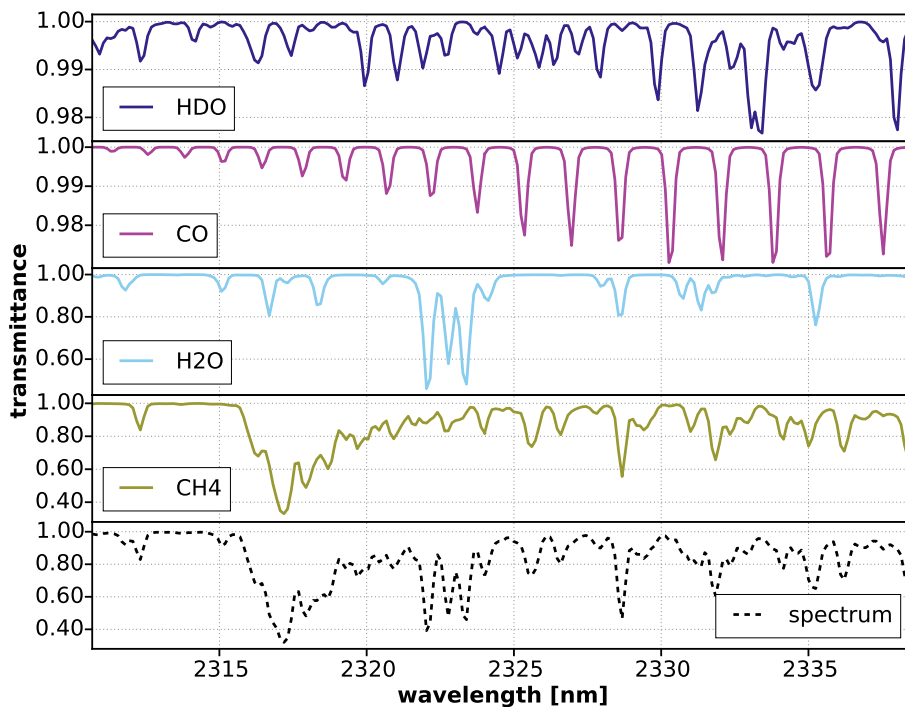


Figure 1. Simulation of atmospheric transmission spectra between 2310.7 and 2338.3 nm with a spectral resolution of 0.25 nm using HITRAN 2008 spectroscopy (Rothman et al., 2003). Panel 1–4: individual atmospheric absorptions of HDO, CO, H₂O, and CH₄. Lower panel: total atmospheric transmission.

SCIAMACHY CO total column measurements (2003–2012)

T. Borsdorff et al.

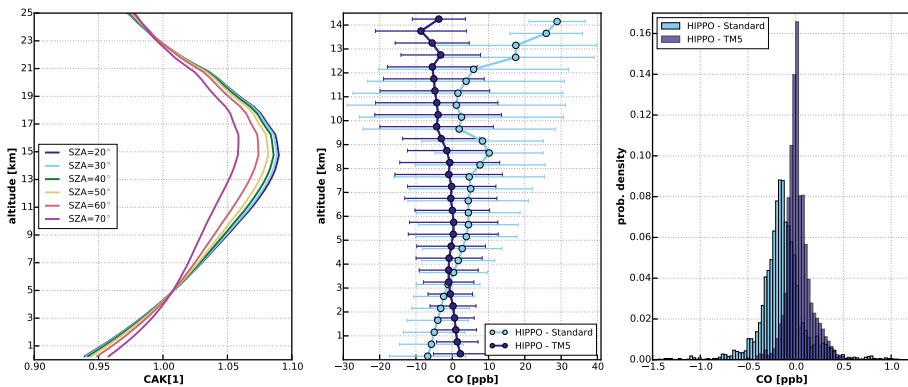


Figure 2. Left panel: SCIAMACHY CO total column averaging kernels for different solar zenith angles (SZA). Middle panel: profile shape difference between HIPPO and TM5/US standard atmosphere. Right panel: probability density distribution of the null space error.

[Title Page](#)[Abstract](#)[Introduction](#)[Conclusions](#)[References](#)[Tables](#)[Figures](#)[◀](#)[▶](#)[◀](#)[▶](#)[Back](#)[Close](#)[Full Screen / Esc](#)[Printer-friendly Version](#)[Interactive Discussion](#)

SCIAMACHY CO total column measurements (2003–2012)

T. Borsdorff et al.

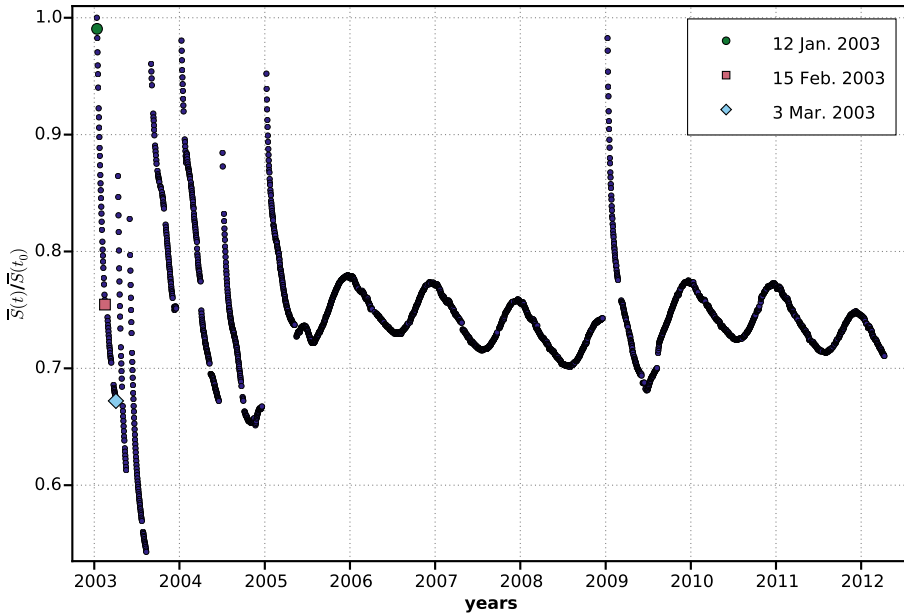


Figure 3. Mean signal of SCIAMACHY's daily sun mean reference (SMR) measurements (2288.72–2383.77 nm) as a function of time relative to 11 January 2003. Three example orbits are marked.

[Title Page](#)[Abstract](#)[Introduction](#)[Conclusions](#)[References](#)[Tables](#)[Figures](#)[|◀](#)[▶|](#)[◀](#)[▶](#)[Back](#)[Close](#)[Full Screen / Esc](#)[Printer-friendly Version](#)[Interactive Discussion](#)

SCIAMACHY CO total column measurements (2003–2012)

T. Borsdorff et al.

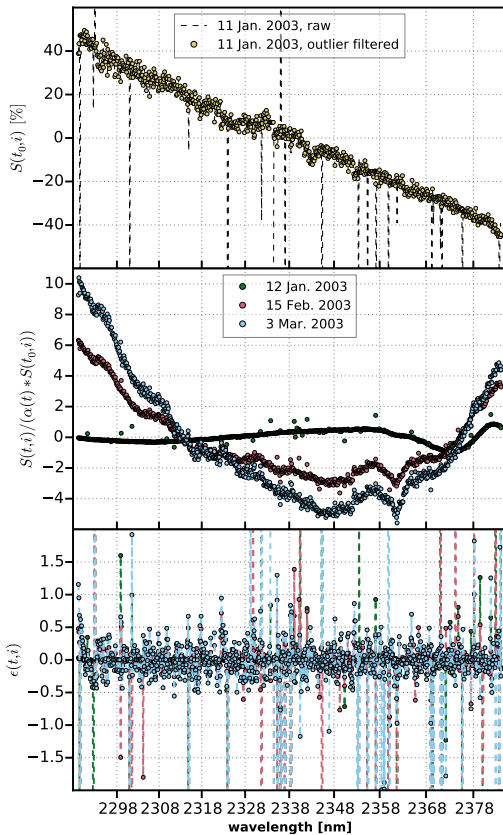


Figure 4. Upper panel: first SMR spectrum of 11 January 2003 expressed as the deviation from its mean signal. This spectrum is used as reference in the following panels. Bad pixels were filtered and interpolated. Middle panel: SMR spectra for three example orbits divided by the reference and smoothed with a running median filter of 10 pixels half width. Lower panel: residuals of the smoothing.

SCIAMACHY CO total column measurements (2003–2012)

T. Borsdorff et al.

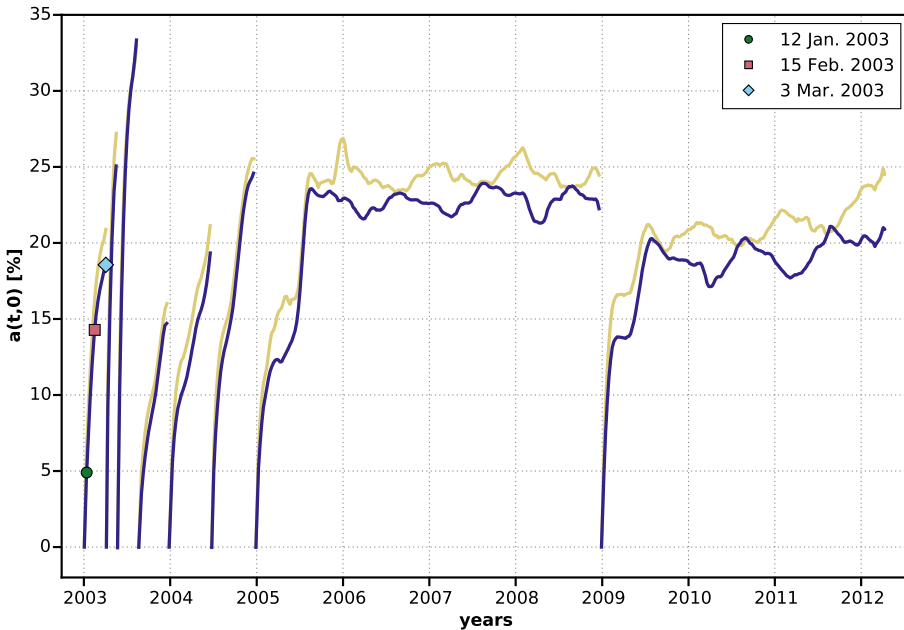


Figure 5. Zero order radiometric offset over time retrieved from cloud-free high albedo SCIAMACHY spectra above the Sahara region (dark blue) and above Australia (yellow). The offset is given in percentage of the mean signal of the spectra and data gaps are interpolated. The three example orbits of Fig. 4 are marked.

[Title Page](#)[Abstract](#)[Introduction](#)[Conclusions](#)[References](#)[Tables](#)[Figures](#)[Back](#)[Close](#)[Full Screen / Esc](#)[Printer-friendly Version](#)[Interactive Discussion](#)

SCIAMACHY CO total column measurements (2003–2012)

T. Borsdorff et al.

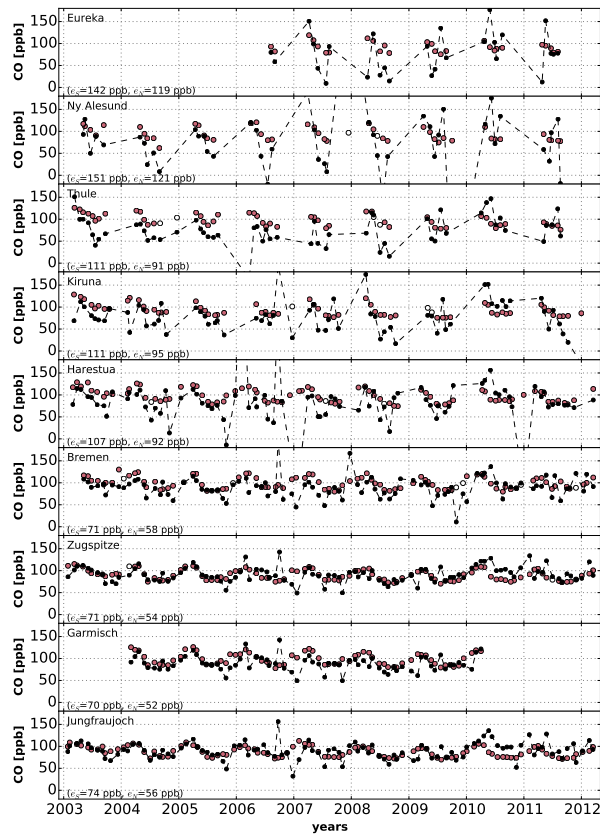
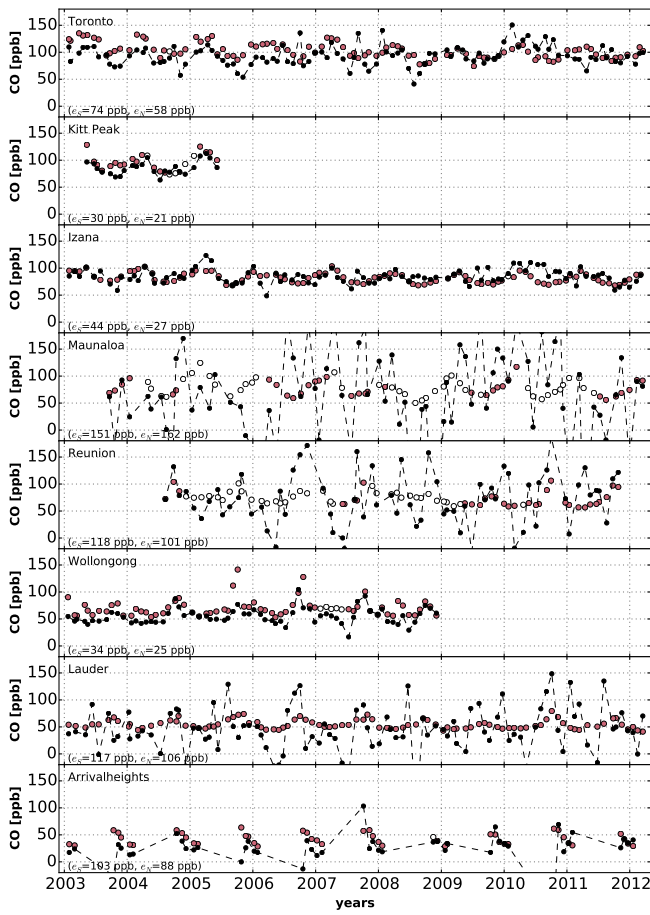


Figure 6a. 30 day medians of CO wet air column averaged mixing ratios measured by SCIAMACHY (black) and at various NDACC-IRWG stations (pink). To derive mixing ratios from the CO columns supplied by NDACC-IRWG we calculated total air columns from the surface pressure per station. Open circles denote interpolated values for periods where no NDACC-IRWG measurements are available.

[Title Page](#)[Abstract](#)[Introduction](#)[Conclusions](#)[References](#)[Tables](#)[Figures](#)[◀](#)[▶](#)[Back](#)[Close](#)[Full Screen / Esc](#)[Printer-friendly Version](#)[Interactive Discussion](#)

SCIAMACHY CO total column measurements (2003–2012)

T. Borsdorff et al.

**Figure 6b.** Continued.

SCIAMACHY CO total column measurements (2003–2012)

T. Borsdorff et al.

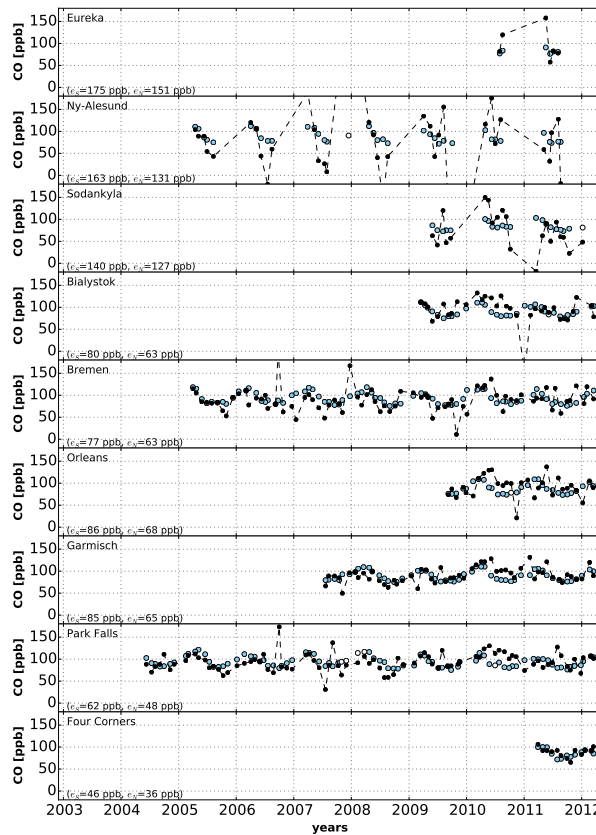
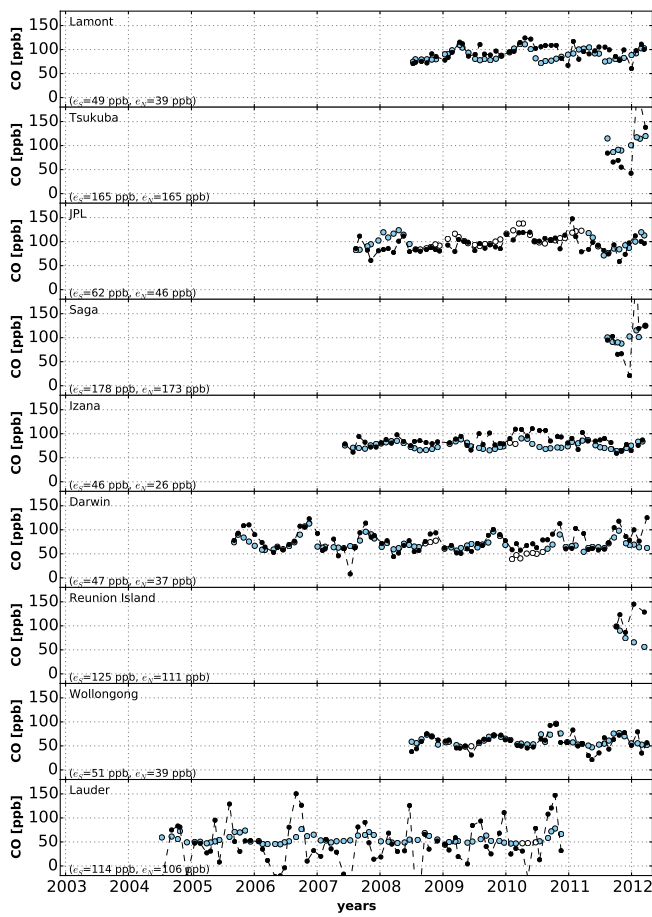


Figure 7a. Same as Fig. 6 but for TCCON measurements indicated in blue. The GGG2014 release of TCCON was used but the stations Ny-Alesund, Bremen, and Four Corners are still based on GGG2012.

[Title Page](#)[Abstract](#)[Introduction](#)[Conclusions](#)[References](#)[Tables](#)[Figures](#)[Back](#)[Close](#)[Full Screen / Esc](#)[Printer-friendly Version](#)[Interactive Discussion](#)

SCIAMACHY CO total column measurements (2003–2012)

T. Borsdorff et al.

**Figure 7b.** Continued.

SCIAMACHY CO total column measurements (2003–2012)

T. Borsdorff et al.

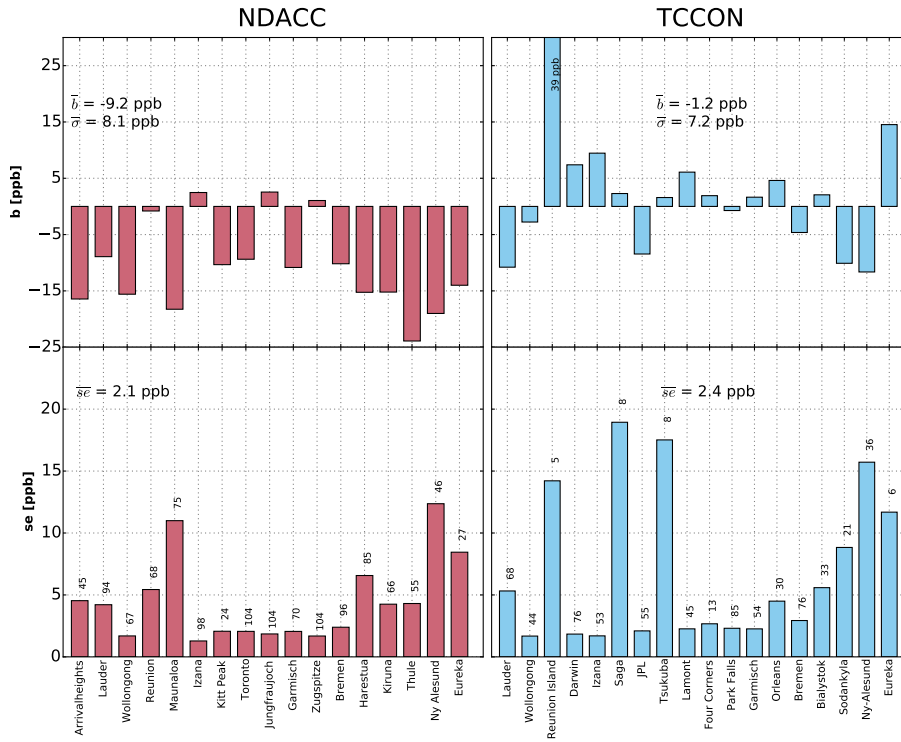


Figure 8. Mean bias (SCIAMACHY–FTS) between measurements of NDACC-IRWG (left panel) and TCCON (right panel) stations with collocated SCIAMACHY CO retrievals and the standard error of the mean bias derived from the 30 day median values shown in the Figs. 6 and 7 (numbers of 30 day medians are indicated above bars). \bar{b} is the global mean bias (average of all station biases weighted by the standard error) and $\bar{\sigma}$ its standard deviation. $\bar{s}e$ is the average of all standard errors.

SCIAMACHY CO total column measurements (2003–2012)

T. Borsdorff et al.

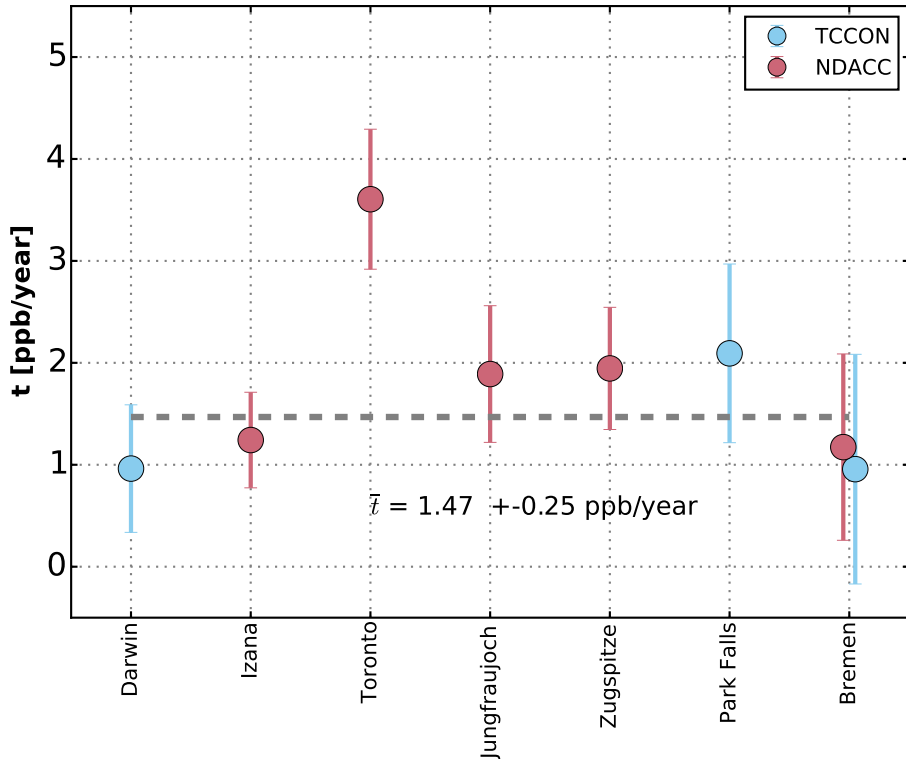
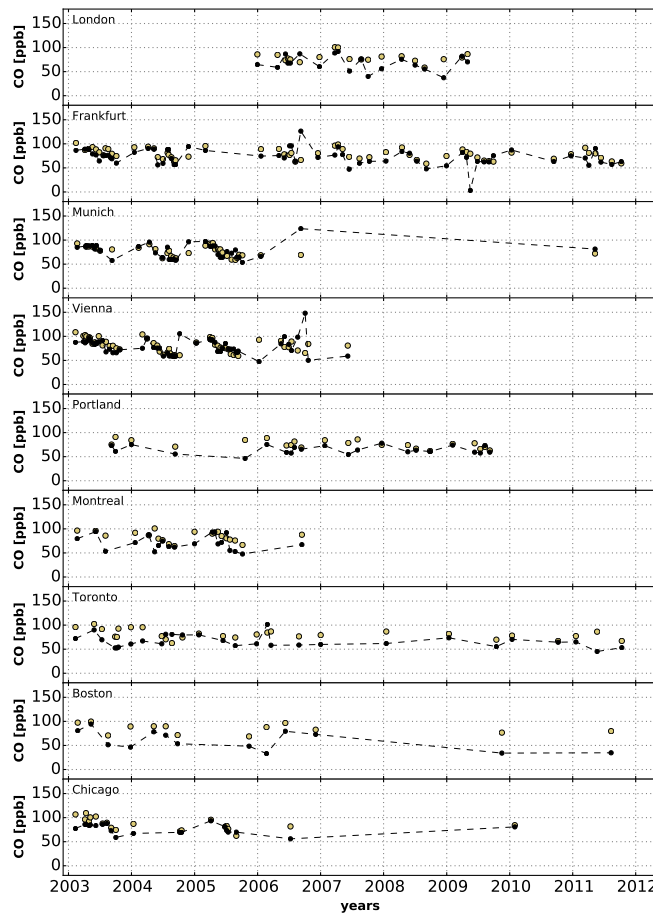


Figure 9. Linear trend t of the mean bias (SCIAMACHY–FTS) derived from 30 day median values shown in the Figs. 6 and 7. Stations with a low retrieval noise that cover the full mission period were selected. Trends are given per station in ppb/year and error bars are the standard deviation. \hat{t} is the average of the trends weighted by the errors excluding measurements at Toronto.

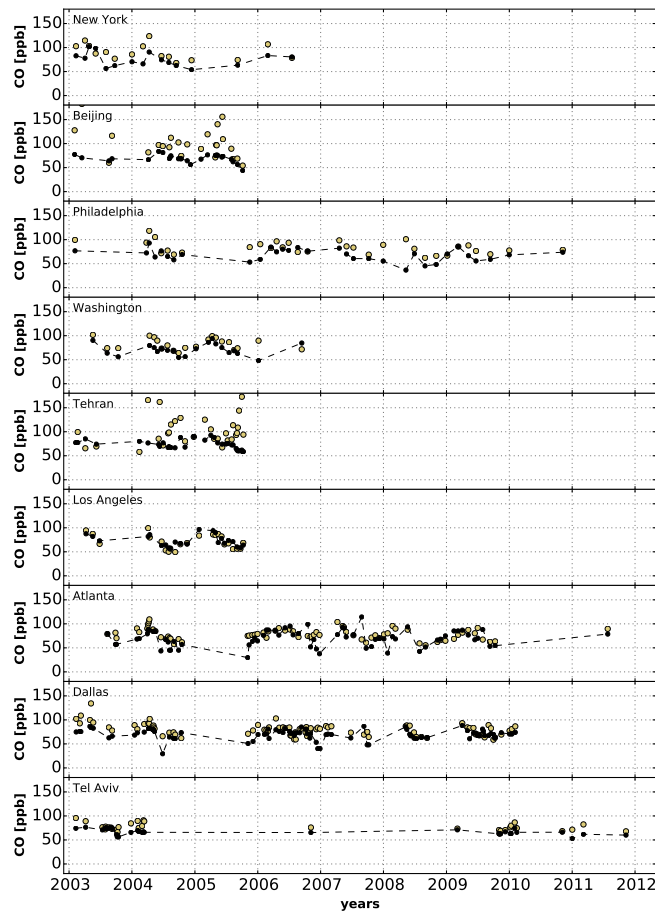
SCIAMACHY CO total column measurements (2003–2012)

T. Borsdorff et al.

**Figure 10a.** Same as Fig. 6 but for MOZAIC/AGOS measurements indicated in yellow.

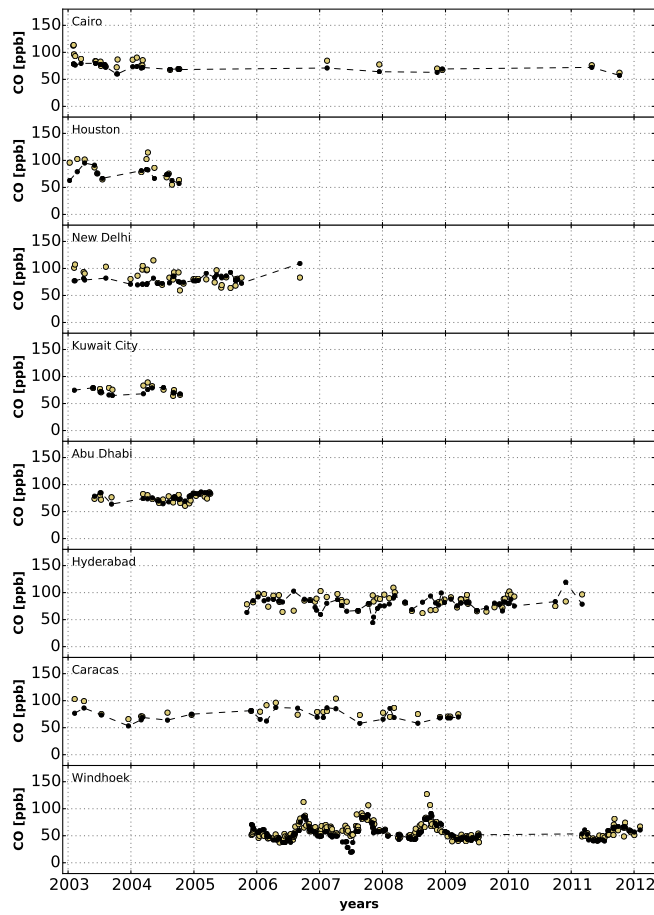
SCIAMACHY CO total column measurements (2003–2012)

T. Borsdorff et al.

**Figure 10b.** Continued.[Title Page](#)[Abstract](#)[Introduction](#)[Conclusions](#)[References](#)[Tables](#)[Figures](#)[◀](#)[▶](#)[◀](#)[▶](#)[Back](#)[Close](#)[Full Screen / Esc](#)[Printer-friendly Version](#)[Interactive Discussion](#)

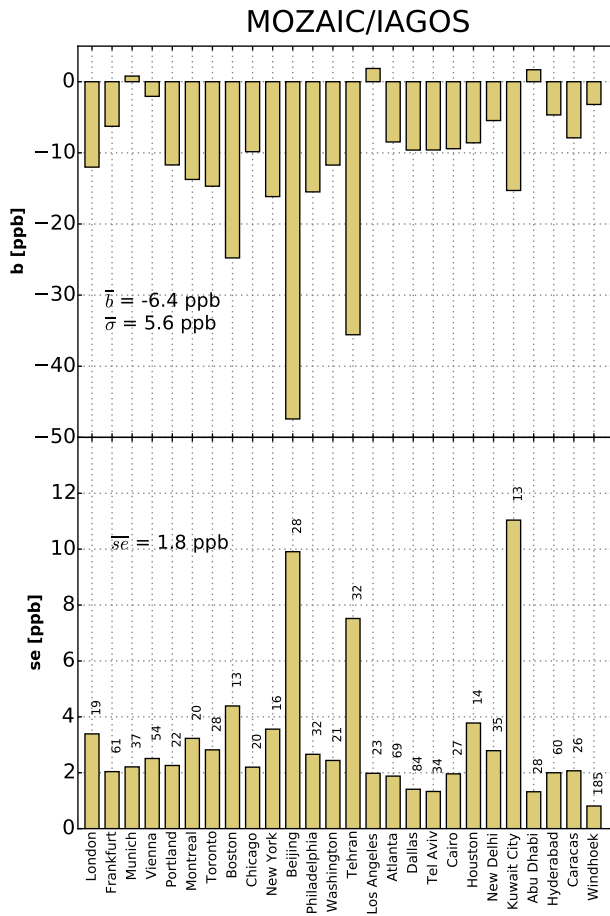
SCIAMACHY CO total column measurements (2003–2012)

T. Borsdorff et al.

**Figure 10c. Continued.**[Printer-friendly Version](#)[Interactive Discussion](#)[Title Page](#)[Abstract](#) [Introduction](#)[Conclusions](#) [References](#)[Tables](#) [Figures](#)[|◀](#)[▶|](#)[◀](#)[▶](#)[Back](#) [Close](#)[Full Screen / Esc](#)

SCIAMACHY CO total column measurements (2003–2012)

T. Borsdorff et al.

**Figure 11.** Same as Fig. 8 but for MOZAIC/AGOS measurements.

SCIAMACHY CO total column measurements (2003–2012)

T. Borsdorff et al.

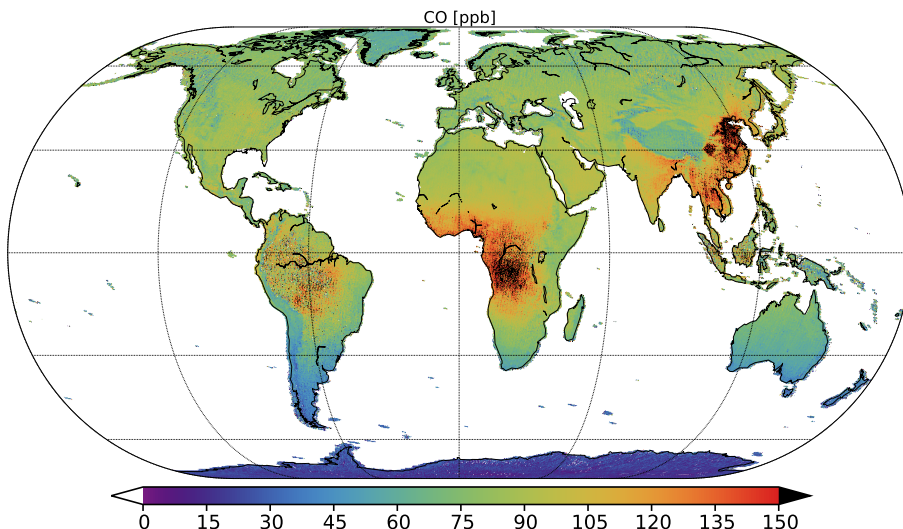


Figure 12. CO wet air column averaged mixing ratios over land and clear-sky scenes. The values are averaged from January 2003 to April 2012 on a cylindrical equal area projection with 180 grid points in latitude and 360 in longitude.

[Title Page](#)[Abstract](#)[Introduction](#)[Conclusions](#)[References](#)[Tables](#)[Figures](#)[◀](#)[▶](#)[◀](#)[▶](#)[Back](#)[Close](#)[Full Screen / Esc](#)[Printer-friendly Version](#)[Interactive Discussion](#)

SCIAMACHY CO total column measurements (2003–2012)

T. Borsdorff et al.

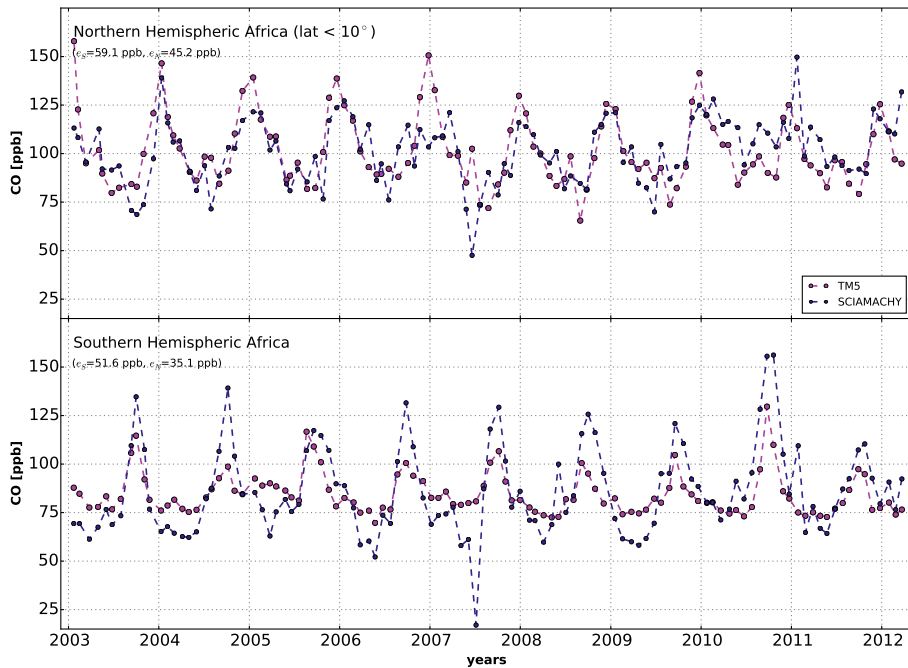


Figure 13. Time series of SCIAMACHY CO wet air column averaged mixing ratios (blue) over Northern and Southern Hemispheric Africa compared with the calculation of the TM5 model (pink). 30 day medians are shown.